Topography of the Calabria subduction zone (southern Italy): Clues for the origin of Mt. Etna

C. Faccenna,[1,2] P. Molin,[1] B. Orecchio,[3,4] V. Olivetti,[1] O. Bellier,[5] F. Funiciello,[1] L. Minelli,[6] C. Piromallo,[7] and A. Billi[2]

Received 18 February 2010; revised 15 September 2010; accepted 28 September 2010; published 11 January 2011.

[1] Calabria represents an ideal site to analyze the topography of a subduction zone as it is located on top of a narrow active Wadati-Benioff zone and shows evidence of rapid uplift. We analyzed a pattern of surface deformation using elevation data with different filters and showed the existence of a long wavelength (>100 km) relatively positive topographic signal at the slab edges. The elevation of MIS 5.5 stage marine terraces supports this pattern, although the record is incomplete and partly masked by the variable denudation rate. We performed structural analyses along the major active or recently reactivated normal faults showing that the extensional direction varies along the Calabrian Arc and laterally switches from arc-normal, within the active portion of the slab, to arc-oblique or even arc-parallel, along the northern and southern slab edges. This surface deformation pattern was compared with a recent high resolution *P* wave tomographic model showing that the high seismic velocity anomaly is continuous only within the active Wadati-Benioff zone, whereas the northern and southwestern sides are marked by low velocity anomalies, suggesting that large-scale topographic bulges, volcanism, and uplift could have been produced by mantle upwelling. We present numerical simulations to visualize the three-dimensional mantle circulation around a narrow retreating slab, ideally similar to the one presently subducting beneath Calabria. We emphasize that mantle upwelling and surface deformation are expected at the edges of the slab, where return flows may eventually drive decompression melting and the Mount Etna volcanism.
Citation: Faccenna, C., P. Molin, B. Orecchio, V. Olivetti, O. Bellier, F. Funiciello, L. Minelli, C. Piromallo, and A. Billi (2011), Topography of the Calabria subduction zone (southern Italy): Clues for the origin of Mt. Etna, *Tectonics*, *30*, TC1003, doi:10.1029/2010TC002694.

1. Introduction

[2] Subduction zones are usually marked by several kilometer deep trenches oceanward often flanked by a few hundred meters high forebulge. The wavelength and amplitude of these topographic features have been successfully modeled both by the bending of an elastic plate [*Turcotte and Schubert*, 1982; *Hager and Clayton*, 1989] and by the flow of a viscous plate [*Zhong and Gurnis*, 1994]. In contrast, the topography of the upper plate shows a more complex signal as it is the product of a variety of processes operating at different spatial scales, including deep crustal underplating, flexural, and tectonic processes commonly active in arc and back arc regions. Over active continental convergent margins, these different contributions are difficult to discern from the simple isostatic component. Such discernment would, in fact, require the exact knowledge of the thickness and density layering of the lithosphere [e.g., *Gvirtzman and Nur*, 1999], including the occurrence of a low-viscosity hydrated mantle wedge [*Billen et al.*, 2003]. Another factor influencing the topography of subduction zones is connected with the plate coupling along the subduction interface [e.g., *Giunchi et al.*, 1996; *Zhong and Gurnis*, 1994; *Wang et al.*, 2003]. In general terms, high coupling or high-convergence velocity along a subduction interface is expected to produce a positive topographic anomaly [*Zhong and Gurnis*, 1994; *Husson and Ricard*, 2004], whereas trench rollback and low coupling are generally associated with topographic sinking of the upper plate, as retrograde slab motion pulls the upper plate down (i.e. "trench suction"; [*Royden and Husson*, 2006; *Husson*, 2006]). However, in the case of a complete decoupling between plates, the overriding plate can also be efficiently lifted up by the inflow of asthenospheric material [*Doglioni et al.*, 2007; *De Franco et al.*, 2008]. Another hypothesized source of topographic deflection is the detachment or breaking of subducting slabs [*Wortel and Spakman*, 2000; *Buiter et al.*, 2002; *Gvirtzman and Nur*, 2001] or the formation of slab windows [*Thorkelson*, 1996; *Guillaume et al.*, 2009]. These processes are considered as efficient sources of rapid upper plate uplift, which would be related to the lithospheric response to unloading, even though this effect could be obscured or retarded by the entrainment of mantle material during the fall of the detached slab portion [*Marotta et al.*, 1998; *Gerya et al.*, 2004]. Moreover, topographic depressions induced by

[1]Dipartimento di Scienze Geologiche, Università Roma Tre, Rome, Italy.
[2]Istituto di Geologia Ambientale e Geoingegneria, CNR, Rome, Italy.
[3]Dipartimento di Fisica, Università della Calabria, Cosenza, Italy.
[4]Dipartimento di Scienze della Terra, Università di Messina, Messina, Italy.
[5]Centre Européen de Recherche et d'Enseignement de Géosciences de l'Environnement, UMR 6635, CNRS, Université Paul Cézanne, Aix-en-Provence, France.
[6]Dipartimento di Scienze della Terra, Sapienza Università di Roma, Rome, Italy.
[7]Istituto Nazionale di Geofisica e Vulcanologia, Rome, Italy.

0278-7407/11/2010TC002694

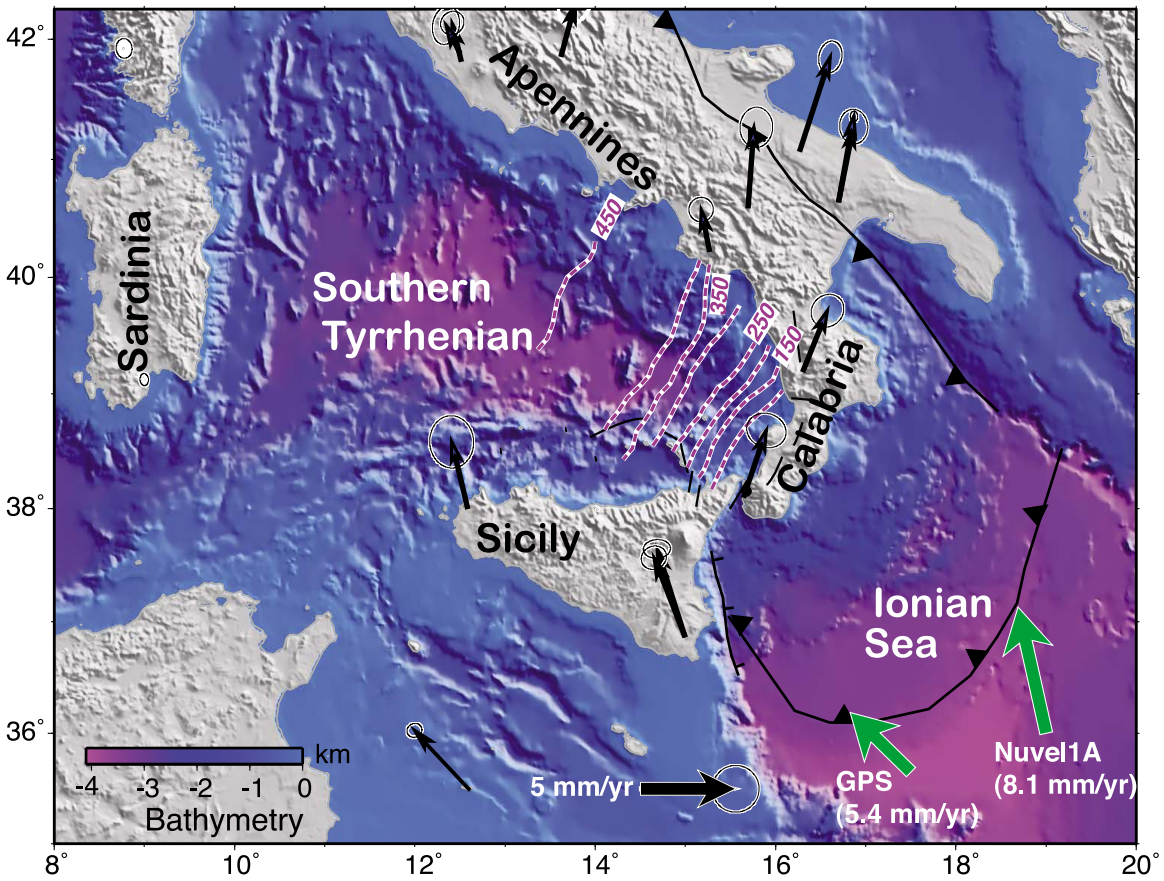

Figure 1. Tectonic setting of the Calabrian subduction zone (modified from *D'Agostino and Selvaggi* [2004]). Geodetic vectors (Eurasia fixed reference frame; *D'Agostino and Selvaggi* [2004]) illustrate the different tectonic regimes of Sicily, whose velocity pattern is consistent with that of Nubia, and of Calabria, whose velocity pattern is not. Note that the main change in the present kinematic setting occurs across the Messina Straits. Purple dashed lines are depth contour lines of the Wadati-Benioff zone.

mantle convection excited by subduction have been reported and modeled for several regions [e.g., *Mitrovica et al.*, 1989; *Gurnis*, 1993; *Zhong and Gurnis*, 1994; *Piromallo et al.*, 1997; *Pysklywec and Mitrovica*, 2000; *Husson*, 2006; *Liu et al.*, 2008]. These remarkable dynamic features associated with subduction are usually represented by the long-wavelength subsidence of continental interiors on the order of a few hundreds of meters or by the formation of deeper than expected back-arc basins [*Hilde and Lee*, 1984; *Husson*, 2006].

[3] The above mentioned processes show that understanding the topography of subduction zones and its dynamics, as well as the cause of mountain belt epirogenic uplift, remains elusive. Documenting and deciphering case histories is therefore fundamental to advance our understanding of the causal relationships between topographic changes and mantle flow in subduction zones.

[4] One challenging instance is the Calabrian subduction zone (southern Italy; Figure 1), where remarkable Quaternary uplift and deformation as well as an active basaltic volcano (Mt Etna) have been so far ascribed to mechanisms as variable as slab break off [*Westaway*, 1993; *Wortel and Spakman*, 2000; *Buiter et al.*, 2002], inflow of asthenospheric material [*Gvirtzman and Nur*, 1999; *Doglioni et al.*, 2007], and lithospheric rebound over a low-friction subduction fault [*Giunchi et al.*, 1996]. Also the source of Etna's magmatism is the subject of controversy. This volcano has been, in fact, related to a deep mantle [*Montelli et al.*, 2004] or to a shallower mantle low-velocity (V_P) source [*Montuori et al.*, 2007] flanking the Ionian slab in the upper mantle. In particular, the molten material feeding Mt Etna probably comes, by suction, from beneath the Nubian plate [*Gvirtzman and Nur*, 1999] through a crustal-tearing structure [*Monaco et al.*, 1997; *Doglioni et al.*, 2001].

[5] In this paper, we present morphological and structural data coupled with high-resolution, deep tomographic images in an attempt to understand and decipher the Quaternary topographic changes of the Calabrian belt and their relationship to the deep mantle structure. Our analysis shows the importance of a three-dimensional (3D) analysis along subduction zones, revealing a remarkable long-wavelength topographic difference between the regions lying over the central and lateral portions of the subducting slab. Based on the presented results and on numerical modeling, we discuss

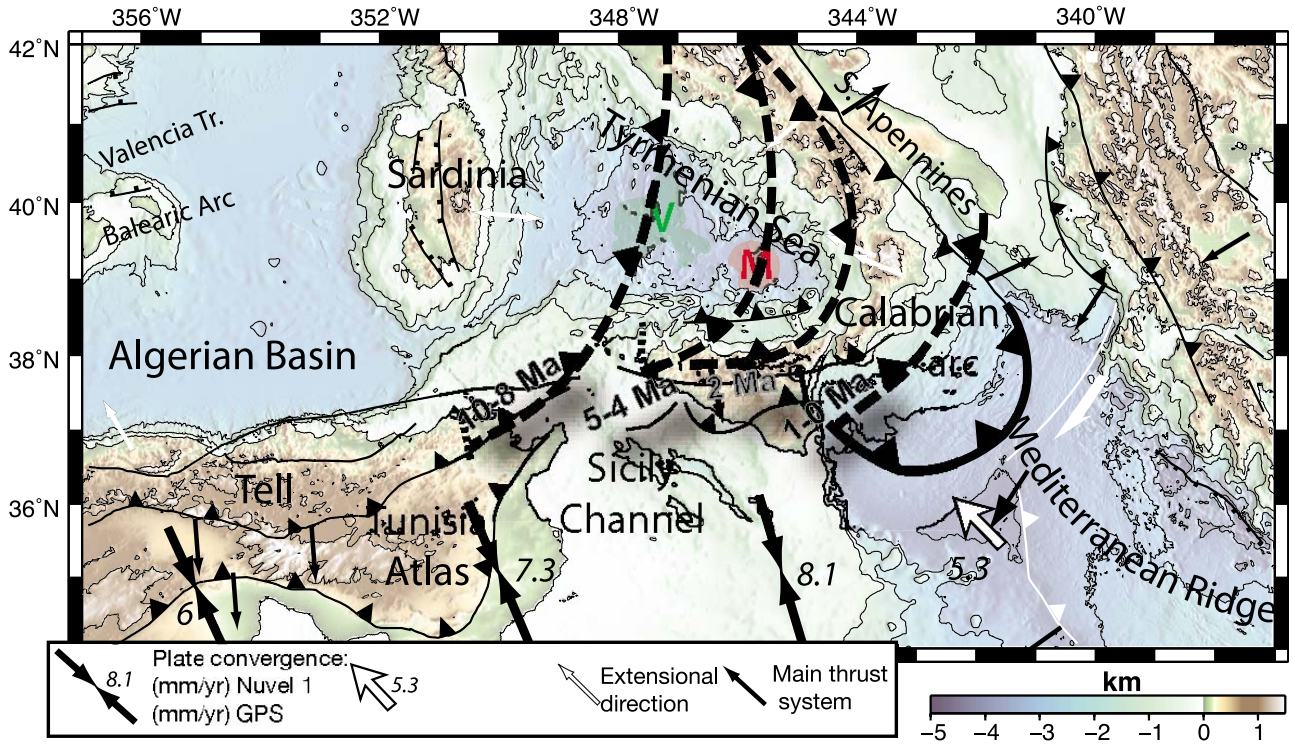

Figure 2. Schematic tectonic evolution of the central Mediterranean region over the past 10 Myr (modified after *Faccenna et al.* [2005]). The trace of the Wadati-Benioff zone at 50 km depth is marked with thick curves. Triangles indicate the sense of subduction. Note the progressive lateral disruption of the subduction zone during the back arc extensional phases. At circa 1 Ma, the system reorganized and a new compressional front developed in the southern Tyrrhenian region (north of Sicily). This front is still active [*Billi et al.*, 2007]. V indicates the Vavilov basin and M indicates the Marsili basin.

a possible model, which may explain the presented surficial and deep evidence.

2. Tectonic Setting

[6] The Calabrian subducting slab presently consists of an approximately 200 km wide and 500 km deep Wadati-Benioff zone [*Anderson and Jackson*, 1987; *Giardini and Velonà*, 1991; *Selvaggi and Chiarabba*, 1995; *Chiarabba et al.*, 2005] dipping toward the northwest at about 70° (Figure 1). The narrow configuration of the slab may have been attained by lateral tearing and mass removal during the last phases of fast slab retrograde migration (i.e., since the Pliocene [*Wortel and Spakman*, 2000; *Faccenna et al.*, 2005]).

[7] Since the Oligocene, the Calabrian trench has rolled back by more than 800 km at an average rate of 2–3 cm/yr [*Malinverno and Ryan*, 1986], producing the opening of the Liguro-Provençal basin first (circa 30–16 Ma; [*Cherchi and Montandert*, 1982; *Burrus*, 1984; *Seranne*, 1999; *Speranza*, 1999]) and, after a short period of quiescence, of the Tyrrhenian basin [*Kasten et al.*, 1988; *Sartori and ODP Leg Sci. Staff*, 1989]. This second Tyrrhenian phase of rollback is likely triggered by the lateral tearing of the Calabrian slab from its western prolongation beneath North Africa [*Carminati et al.*, 1998; *Faccenna et al.*, 2004, 2005] (Figure 2). Spreading in the Tyrrhenian occurred with two distinct episodes; the Vavilov basin (~4–3 Ma) and the Marsili basin (~2–1 Ma) with a sharp decrease of the subduction zone width [*Guillaume et al.*, 2010]. The Marsili basin (Figure 2) opened at a fast rate probably during the fast 15°–25° clockwise rotation of the Calabrian Arc [*Speranza et al.*, 2000; *Cifelli et al.*, 2007b; *Chiarabba et al.*, 2008; *Nicolosi et al.*, 2006].

[8] The present day tectonic configuration of the Tyrrhenian basin was achieved after circa 1–0.7 Ma (Figures 1 and 2), when the plate boundary system reorganized to accommodate the Africa-Eurasia convergence [*Goes et al.*, 2004]. After the locking of the Apennines and southern Sicily (Gela nappe) thrust systems [*Argnani et al.*, 1987; *Casero and Roure*, 1994; *Patacca et al.*, 1990; *Mattei et al.*, 2004], compressional displacements remained active offshore Calabria [*Doglioni et al.*, 1999] and resumed along an active belt located in the southern Tyrrhenian region [*Billi et al.*, 2007] (Figure 1), and a diffuse transform zone formed in northeastern Sicily and the northwestern Ionian region to accommodate the remaining active portion of the slab beneath Calabria [*D'Agostino and Selvaggi*, 2004; *Goes et al.*, 2004; *Billi et al.*, 2006].

[9] The reorganization of the plate boundary is marked by two main processes. First, as discussed below, Calabria started to uplift at this time. Second, at about 0.5 Ma, tho-

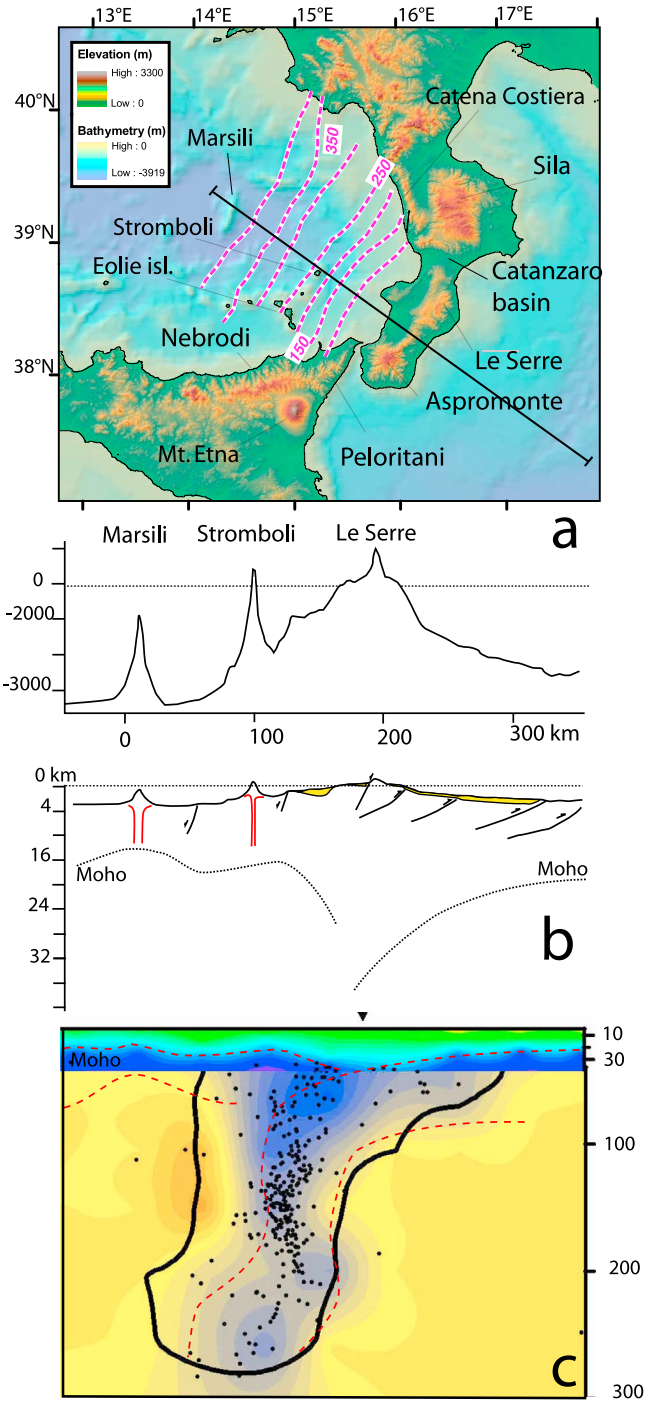

Figure 3. Bathymetry, crustal thickness, and mantle seismic anomaly distribution [*Neri et al.*, 2009] along a NW–SE profile across central Calabria. Calabria stands between two deep floor basins, producing an asymmetric bell-shaped topography. Crustal thickness is from receiver function [*Piana Agostinetti and Amato*, 2009] and seismic [*Suhadolc and Panza*, 1989] data. Note the sharp curvature of the subvertical slab.

leiitic magmas started to erupt, building up the large Mt Etna shield volcano, which is located right on top of the western edge of the Calabrian subduction zone (Figures 1 and 2).

3. Surface Deformation

3.1. Regional-Scale Topographic Features

[10] A cross section perpendicular to the subduction zone shows that the Calabrian belt is characterized by a bell-shaped morphology, flanked on both sides by 2–3 km deep abyssal plains floored by oceanic or transitional crust [*Catalano et al.*, 2001] (Figure 3b). The Ionian, eastern flank shows a gentle dip slope (<1°). Conversely, along the Tyrrhenian side, the slope is steeper and marked by stepwise escarpments related to normal faults. The emerged portion of the belt is narrow, 50–100 km wide (Figures 4a, 4c–4e). Here, the landscape is steep, rising to an altitude of more than 1000 m and peaking at Mt Botte Donato (1928 m of elevation) in the Sila Massif. A comparison with the deep crustal structure shows that the divide is located in the region with the largest crustal thickness (Figure 3b) [*Piana Agostinetti et al.*, 2009] and just to the back of the steep subduction zone (Figure 3c).

[11] We analyzed the topographic signal of the entire Calabrian Arc by smoothing the digital topography by a low pass filter at three different wavelengths (100, 200, and 300 km). This method is useful to isolate regional-scale features from short wavelength topographic features supported by tectonic or elastic flexure [*Wegmann et al.*, 2007; *Roy et al.*, 2009]. Before digital elevation model (DEM) filtering, we removed the Mt Etna positive signal, replacing it with the average elevation of the adjacent plain (400 m). The obtained maps (Figures 4a) show a regional trend of the narrow and elongated Calabrian Arc between the two negative signals provided by the Tyrrhenian and Ionian basins located to the northwest and southeast, respectively. The topographic signal along the strike of the arc is non-cylindrical, being marked by a relative depression occurring in the center of the arc (i.e., over Le Serre, Aspromonte, and Peloritani Mts.). This relative depression is a robust feature regardless of the used wavelength (Figure 4a) and is confirmed by filtering short wavelengths (~50 and ~100 km) from the along-strike swath profile (Figures 4e, 4f). On average, the elevation difference increases with the low-pass threshold, from about 500 m for a 100 km wavelength, to >600–800 m for larger wavelengths.

[12] To illustrate the topographic pattern along the Calabrian Arc and Sicilian Maghrebides belt, we also show five swath profiles, two along-strike and three perpendicular to the chain (Figure 4). The Sila Massif is characterized by a low relief upland morphological surface, 40 km wide, standing at an average elevation of 1200 m (Figures 4b, 4f), and interpreted as a relict of an old landscape developed in stable, base level conditions [*Dramis et al.*, 1990; *Molin et al.*, 2004]. Its age is not yet determined, but early Miocene (between circa 30 and 15 Ma) fission track ages [*Thomson*, 1998] indicate that the erosion rate has been limited. The origin of the low-relief landscape could be then as old as Tortonian time, which is the age of the first marine deposits tilted on top of the crystalline basement [*Henderson*, 1970;

Guérémy, 1972]. The Sila Massif flanks are asymmetric, the western flank being steeper than the eastern one (Figure 4b). The western flank is probably controlled, at least in the southern portion, by active normal faulting [*Galli and Bosi*, 2003; *Molin et al.*, 2004; *Tansi et al.*, 2005; *Spina et al.*, 2009] (Figure 4b), which induces a general eastward tilt of the massif. The emerging fault system is located along the western side of the Crati basin, a half graben bounded by an east-dipping normal fault system growing from the Tortonian onward [*Cifelli et al.*, 2007a] (Figure 4b). The steep southern flank of Sila corresponds to a normal fault system that borders the Catanzaro Trough to the north [*Monaco and Tortorici*, 2000; *van Dijk et al.*, 2000; *Galli and Bosi*, 2003; *Tansi et al.*, 2007] (Figure 4f). Moving southward, the long-wavelength topography of the Sila Massif disappears and the emerged land portion gets narrow, whereas the mean topography of the belt (Le Serre) only exceeds 900 m (Figures 4c, 4f). The relief of Le Serre is bounded to the west by large, active normal faults facing the Tyrrhenian Sea (Figure 4c). Its asymmetric shape and, in particular, the slope of its eastern flank indicate that at least part of the relief is related to flexural fault footwall uplift [*Jacques et al.*, 2001]. Further south, the belt topography progressively rises again, forming the Apromonte Massif, where the traces of a flat morphological paleosurface on top are still preserved at elevations of 1200–1400 m [*Dumas et al.*, 1982; 1988; *Barrier et al.*, 1986; *Miyauchi et al.*, 1994] (Figure 4d, 4f). Toward the south, the Aspromonte rapidly decreases down to the Messina Straits (Figure 4f). The Aspromonte range is bordered to the west by a system of west-dipping normal faults that control the formation of the Messina basin [*Bousquet et al.*, 1980; *Ghisetti*, 1992; *Tortorici et al.*, 1995; *Monaco and Tortorici*, 2000 and references therein; *Galli and Bosi*, 2002; *Catalano et al.*, 2003, 2008]. The Messina trough interrupts the continuity of the arc and is constituted by a narrow and deep NNE-striking topographic depression filled by Lower Pleistocene to Holocene sedimentary deposits [*Jacques et al.*, 2001]. The western flank of the Messina trough is composed of a NNE-SSW-trending fault, responsible for the 1908 destructive earthquake [*Valensise and Pantosti*, 1992; *Monaco and Tortorici*, 2000; *Catalano et al.*, 2003]. The swath profile along the strike of the Sicilian Maghrebides belt shows a topography rising toward the west (Figure 4e). The elevation rises from the Peloritani Mts., which stand at a mean elevation of less than 500 m, to the Nebrodi Mts., which reach a maximum altitude of ~1000 m to the west of the Tindari fault system [*Lanzafame and Bousquet*, 1997; *Billi et al.*, 2006]. With the local interruption of the Cefalù fault system, the topography progressively decreases toward the west (i.e., in northwestern Sicily).

[13] In synthesis, the Calabrian Arc topography is characterized by two highs, namely Sila and Nebrodi, separated by the less elevated Le Serre range.

3.2. Quaternary Uplift

[14] Both the Tyrrhenian and the Ionian sides of Calabria are characterized by spectacular marine terraces and associated deposits. For instance, littoral deposits of the early-middle Pleistocene age are exposed at elevations of up to almost 1400 m [*Ciaranfi et al.*, 1983; *Ogniben*, 1973]. Many studies have been carried out to define the ages of the Calabrian terraces and to derive the related uplift rates [*Pirazzoli et al.*, 1997; *Stewart et al.*, 1997; *Antonioli et al.*, 2006a, 2009]. The oldest marine terrace has been detected on top of Aspromonte and Le Serre and has been referred to the early Pleistocene time, providing an average uplift rate of about 1 mm/yr [*Barrier et al.*, 1986; *Miyauchi et al.*, 1994; *Balescu et al.*, 1997].

[15] In Calabria, the Marine Isotopic Substage (MIS) 5.5 terraces, commonly referred to as the Tyrrhenian/Eutyrrhenian stage, are well-mapped and constrained [*Cosentino and Gliozzi*, 1989; *Ferranti et al.*, 2006; *Robustelli et al.*, 2009]. According to deep-sea high-resolution oxygen isotopic stratigraphy, MIS 5.5 occurred between 132 and 116 ka [*Stirling et al.*, 1995; *Chapell et al.*, 1996; *Shackleton*, 2000]. In the Mediterranean, the sea level during this stage stood at an elevation of approximately 6 ± 3 m [*Lambeck et al.*, 2004; *Dumas et al.*, 2005]. Coastal deposits with warm faunal assemblages ("fauna senegaliensis" of *Gignoux* [1913]), including molluscs such as the index fossil *Strombus bubonius*, are typical of the MIS 5.5 terraces. In some cases, the attribution of these marine terraces to MIS 5.5 is based on radiometric dating [*Westaway*, 1993; *Bordoni and Valensise*, 1998; *Catalano et al.*, 2003; *Ferranti et al.*, 2006; *Bardají et al.*, 2009].

[16] Figure 5 shows the elevation of the MIS 5.5 terraces mainly based on the available dataset, as reviewed by *Bordoni and Valensise* [1998] and *Ferranti et al.* [2006]. Discrepancies of a few meters between different sources on the local elevation of the MIS 5.5 terraces in Calabria are not relevant here as the main aim consists of detecting differential uplifts over length scales of 50 km or more (see section 3.1). The main observations and inferences on the distribution of the MIS 5.5 terraces in Sicily and Calabria (Figure 5) are five-fold.

[17] 1. To the north of Catanzaro basin, the terrace altitude on the Tyrrhenian side of Calabria is usually lower than that on the Ionian side (Figure 5). Exceptions to this rule occur in southern Calabria (e.g., the Capo Vaticano area). The altitude discrepancy between the Tyrrhenian and Ionian terraces can be partly explained by the presence, on the Tyrrhenian side, of normal faults that down faulted the terraces during the uplift of Calabria [*Monaco and Tortorici*, 2000; *Jacques et al.*, 2001; *Catalano et al.*, 2003]. In contrast, except for the Crotone promontory, the terraces on the Ionian side of Calabria have not been affected by normal faults. It follows that data from this side of Calabria (Ionian) may provide a more reliable evidence for the large-scale uplift process than the data coming from the opposite side (Tyrrhenian), where normal faulting could have locally affected the elevation of the studied terraces.

[18] 2. Elevation peaks of terraces occur in two areas, the Aspromonte-Peloritani area (110–160 m) and the northern Sila–southern Pollino area (104–145 m). In both areas, the uplifted region extends over some tens of kilometers (Figure 5b).

[19] 3. The highest elevation of the MIS 5.5 terrace is recorded along both coasts of the Messina Straits. These data are consistent with average uplift rates greater than 1 mm/yr.

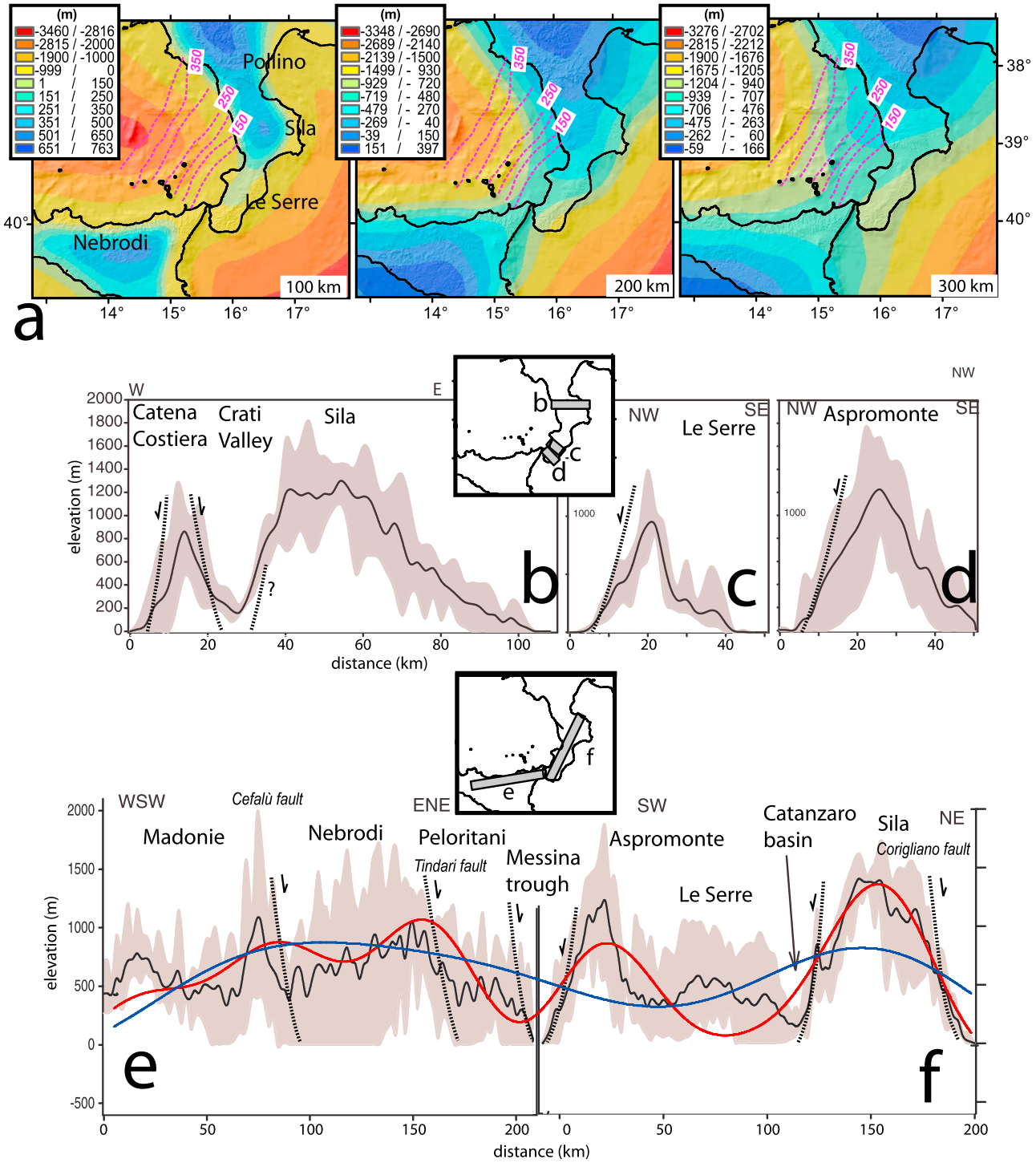

Figure 4. Topographic features of the Calabrian arc. (a) Filtered topography at 100, 200, and 300 km wavelength (topography of Mt Etna is removed from calculation) from a digital elevation model (DEM) derived from the Shuttle Radar Topography Mission data (courtesy of the Global Land Cover Facility, University of Maryland) with a pixel resolution of 30 arcsec (~1500 m). Note the presence of the relative high beneath Sila-Pollino and Sicily, just positioned on the sides of the slab (purple curves). (b, c, d) Swath profiles perpendicular and (e, f) parallel to the strike of the arc with maximum, minimum, and mean elevation. Red and blue curves result from filtering raw topography with cutoff wave lengths of ~50 and ~100 km, respectively.

Although in the Messina Straits area, the elevation of the MIS 5.5 terrace may have been locally influenced by footwall uplift along major faults [*Catalano et al.*, 2003; *Ferranti et al.*, 2006; *Tortorici et al.*, 2003], the decay in elevation toward both the west and the south suggests the presence of a larger wavelength regional swelling.

[20] 4. Terraces on the northern flank of the Sila Massif also show high elevations. In particular, elevation increases northward along the axis of the massif (i.e., from 104 to 130 m), thus depicting a regional bulge. This evidence indicates that the low altitude values (84–110 m) observed at Crotone cannot be taken as representative because of the large distance from the range axis and the presence of east-dipping normal faults in the Crotone basin [*Zecchin et al.*, 2004].

[21] 5. Over Le Serre Massif, which is a narrow massif where the terraces are close to the range axis, the MIS 5.5 terraces stand at an elevation of circa 90 m, which is low with respect to the elevation of isochronous terraces on the Sila and Aspromonte massifs (Figure 5).

[22] In synthesis, the distribution of the MIS 5.5 terraces indicates regional uplifts with differential rates, with the largest elevations in the Messina Straits area and in the northern side of the Sila-southern Pollino massifs. The Le Serre range, in contrast, is characterized by minimum elevations and rates of the MIS 5.5 terraces.

3.3. Recent and Active Faults

[23] Calabria and northeastern Sicily are among the most active (tectonically and seismically) areas of the Mediterranean region. Several studies have been done to identify and map the active faults in these two areas [*Cello et al.*, 1982; *Tortorici et al.*, 1995; *Monaco et al.* 1997; *Monaco and Tortorici*, 2000; *Jacques et al.*, 2001; *Galli and Bosi*, 2002, 2003; *Billi et al.*, 2006, 2007, 2010; *Catalano et al.*, 2008; *Galli et al.*, 2008; *Spina et al.* 2007; 2009]. We based our field structural analyses on these previous studies and fault mapping.

[24] We conducted field structural analyses on the main recent faults exposed in Calabria and northeastern Sicily to define their geometry and last slip direction. The analysis was applied to all faults showing evidence of Quaternary activity (i.e., faults not necessarily active). To do this, we measured the orientations of fault planes and related recent slip vectors inferred from slickenlines, striae, grooves, and, in some places, calcite or quartz fibers, for a total of more than 200 slip vector measurements. We also analyzed cross-cutting and over-printing relationships to infer the relative timing of slip events over fault planes. The results of our fault mapping and related kinematic analysis are summarized below and in Figure 6.

[25] In the Crati Valley (northern Calabria, Figure 6a), an en echelon set of normal faults is nicely exposed. *Cello et al.* [1982] and *Tortorici et al.* [1995] describe the morphological features of this fault system along with structural data indicating overall oblique dextral kinematics. These faults have been active since late Miocene, as shown by the growth strata of this age [*Cifelli et al.*, 2007a]. The fault zone is characterized by two sets of triangular facets that indicate recent normal-faulting activity. At one site, these faults cut Upper Pleistocene cones and fluvial terraces. Kinematic analyses conducted over fault planes exposed at four measurement sites (5, 7, 8, and 10) partly confirm the structural results of *Tortorici et al.* [1995] and *Spina et al.* [2009]. The major fault shows normal to oblique dextral kinematics; however, at two sites (5 and 10), we also found evidence for a younger set of striae superimposed on the previous one, indicating normal to oblique sinistral motion.

[26] The Sila massif is characterized by well-exposed fault planes along its northern and southern sides, and within the massif itself (Figure 6b). To the north, close to Corigliano (site 3), the northern side of the Sila massif is bordered by a well-exposed fault plane marking the contact between basement units and Upper Pliocene to Upper Pleistocene deposits [*Tortorici*, 1981; *Ciaranfi et al.*, 1983; *Knott and Turco*, 1991; *Moretti*, 2000; *Van Dijk et al.*, 2000]. Slickensides along the main fault plane show normal to oblique dextral motion. On the Sila massif plateau, *Galli and Bosi* [2003] describe and map a NNW-trending fault zone (the Lake fault system). Their analyses within paleoseismological trenches show recent (i.e., Holocene) slip along this fault. *Spina et al.* [2007] performed a kinematic analysis along the same fault showing overall oblique sinistral kinematics. To the south of the Sila massif and north of Lamezia Terme, the Catanzaro basin is bordered by a west-striking fault marking the contact between basement units and recent deposits. Kinematic analysis along this fault (sites 13 and 15; Figure 6) reveals normal dip-slip displacements.

[27] Moving toward the south, the Le Serre range is flanked to the west by the Serre-Cittanova normal fault system, which bounds, to the east, the Mesima and Gioia Tauro basin [*Tortorici et al.*, 1995; *Monaco and Tortorici*, 2000; *Jacques et al.*, 2001; *Galli and Bosi*, 2002]. The main fault planes, which are morphologically very clear (i.e., from aerial view), crop out only at a few sites (Figure 6c). We analyzed the Serre-Cittanova fault close to the trench site studied by *Galli and Bosi* [2002]. At sites 21, 22, and 24 (Figure 6), kinematic indicators show normal dip-slip displacement for the Serre-Cittanova fault. To the southwest, the prolongation of the Serre-Cittanova fault splits into horsetail segments located close to the Messina trough. One of these segments (the S. Eufemia fault) is characterized by normal to left-lateral oblique slip displacements (site 23), as also reported by *Tortorici et al.* [1995]. Moving toward the west, the southern side of the Capo Vaticano promontory is bounded by a west-striking fault, the Coccorino fault [*Tortorici et al.*, 2003] characterized by normal displacements (site 19).

[28] At Tindari, in northeastern Sicily (Figure 6d), a regional NNW-striking system of right-lateral strike-slip faults is reactivated by normal dip-slip and transtensional motions [*Billi et al.*, 2006], similar to what is observed in the area between Cefalù and Mt Etna [*Billi et al.*, 2010]. On the eastern flank of Mt Etna, north-striking faults are characterized by normal to right-lateral transtensional displacements [*Monaco et al.*, 1997].

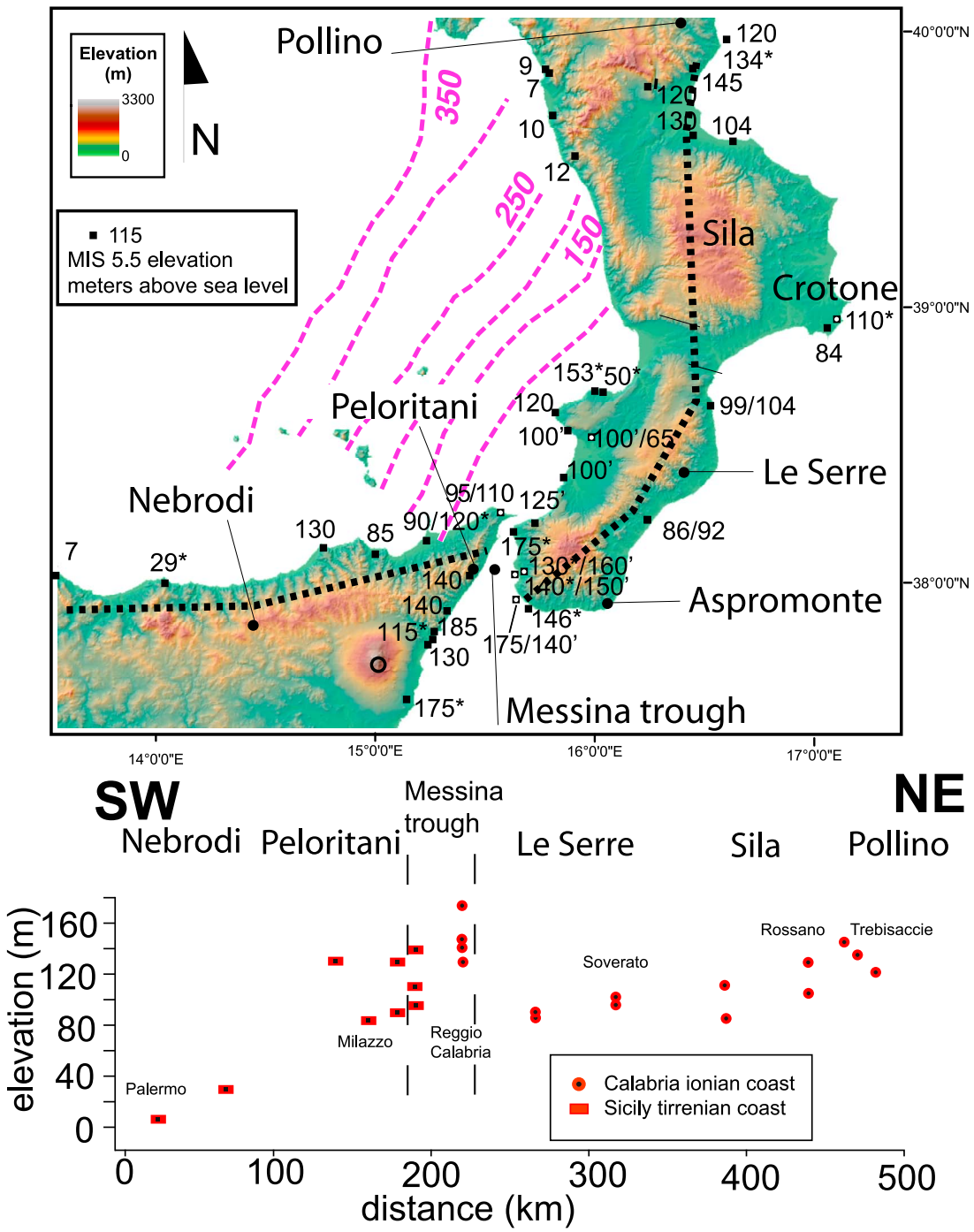

Figure 5. Elevation distribution of the MIS 5.5 marine terraces in northeastern Sicily and Calabria. Two adjacent numbers denote elevations from different sources. Asterisks are for terraces dated through paleontology, aminostratigraphy, thermoluminescence, and U/Th chronology. Diagram shows the elevation of the MIS 5.5 marine terraces projected along a transect from northeastern Sicily and Calabria. Minimum values correspond to the active portion of the slab, whereas maximum values correspond to the Messina region.

[29] In synthesis, the orientation of slip indicators (Figure 6e) indicates that strain field is variable along the arc. The fault pattern at Le Serre is constituted by NNE-striking fault system under a NW extensional field [*Tortorici et al.*, 1995]. North of Catanzaro basin, the most recent slip on the Crati fault system, the Lake fault system [*Galli et al.*, 2007; *Spina et al.*, 2007] and the Corigliano and Lamezia faults develop under an overall ENE-trending to NE-trending

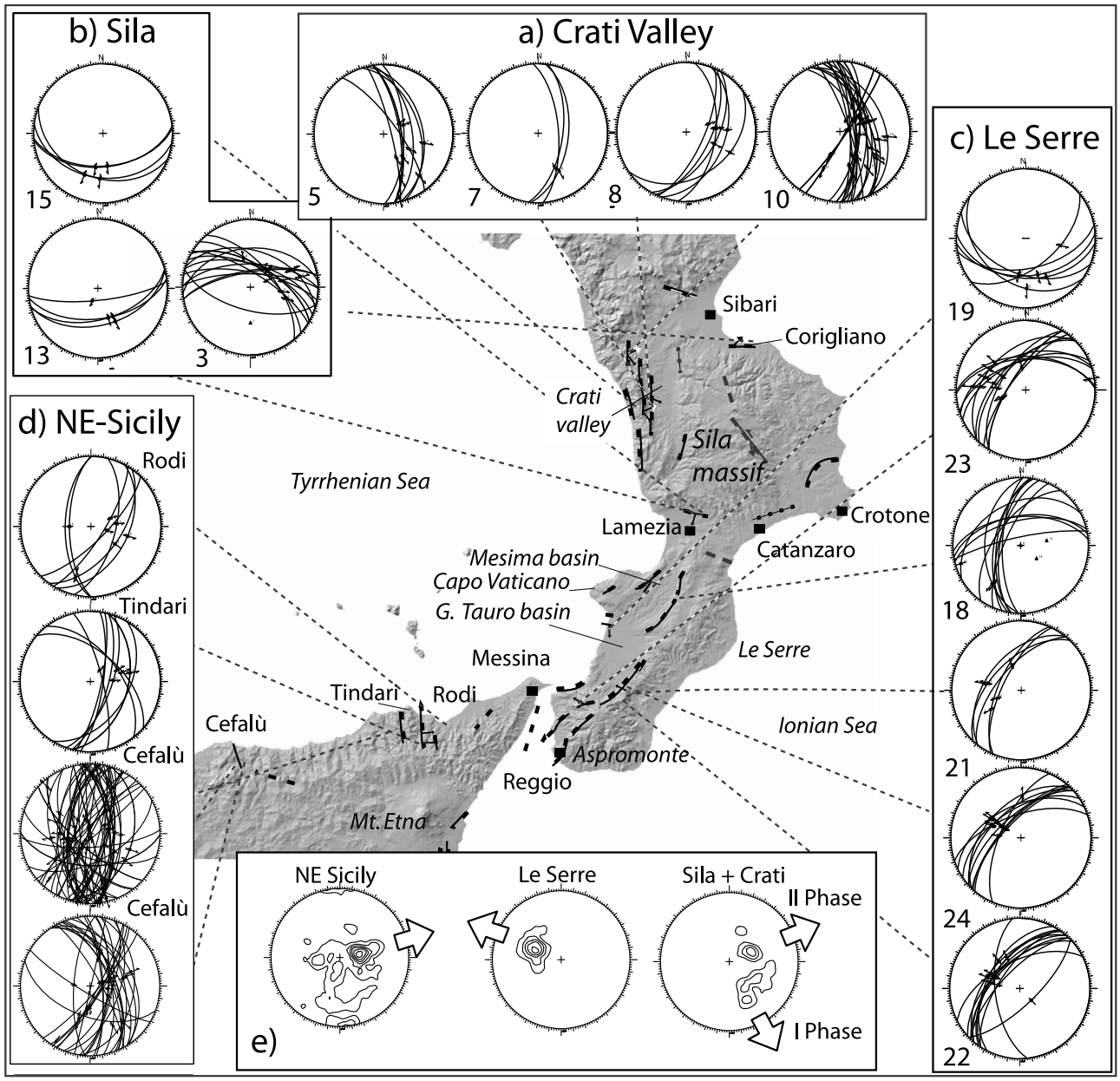

Figure 6. Map of studied faults and related mesostructural data (i.e., attitudes of faults and kinematic indicators) plotted on lower hemisphere Schmidt nets. Sense of fault slip is indicated by arrows. Most analyzed faults are normal or oblique. The fault population is divided into (a) Crati valley, (b) Sila massif, (c) Le Serre, and (d) NE Sicily areas. (e) Contour lines (Kalsbeek net, lower hemisphere) of the slickenlines of normal–oblique faults measured in the different regions. Arrows show the deduced average slip directions along the normal faults. Note that the mean direction of slip (i.e., extension) changes moving from NE Sicily to Le Serre and the Sila-Crati region. The latter shows two population of slickenside, with the younger one striking ENE, similar to the one of NE Sicily. In the Le Serre region mean slip direction strikes, conversely, toward the NW.

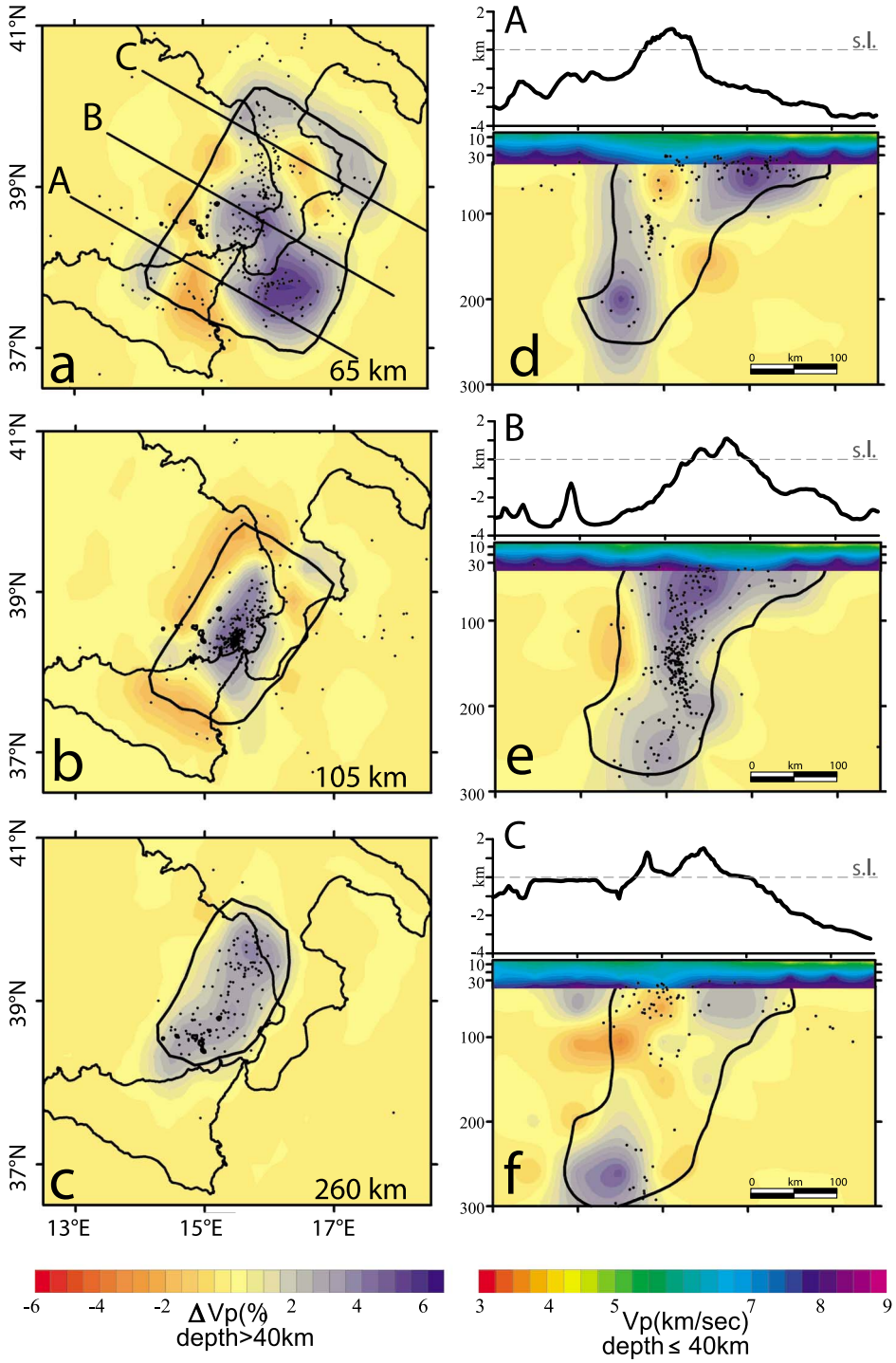

Figure 7. A *P* wave tomographic model of Calabria and northeastern Sicily based on a high-resolution regional array (modified from the model of *Neri et al.* [2009]). At depths deeper than 40 km colors represent deviation in percentage of *P* velocity from the ak135 model [*Neri et al.*, 2009]. Horizontal slices at depths of (a) 65, (b) 105, and (c) 260 km illustrate the horizontal width of the slab, which is only about 100 km at shallow levels and slightly larger at deeper levels. Cross sections show the geometry of the slab mantle system along (d) northern and (e) central Calabria, and (f) northeastern Sicily. The slab appears continuous (nondetached) only in central Calabria, whereas to the north and south, the slab is separated from its deeper portion by a low velocity anomaly. Black lines contour the zone where spread function values are not larger than 3.25.

extension. In northern Sicily the most recent fault system is undergoing an ENE-trending to east-trending extension.

4. Deep Structure: Upper Mantle Tomography

[30] Several regional tomographic studies have recently imaged the upper mantle structure beneath the central Mediterranean [*Lucente et al.*, 2006; *Wortel and Spakman*, 2000; *Piromallo and Morelli*, 2003; *Montuori et al.*, 2007; *Chiarabba et al.*, 2008; *Caló et al.*, 2009]. Local earthquake tomography with data from intermediate and deep events [*Neri et al.*, 2009] provides a new and detailed distribution of the velocity structure in the 40–260 km depth range beneath the Calabrian arc. This high resolution tomography shows the velocity anomaly distribution (in terms of percentage velocity variation with respect to the ak135 velocity model of *Kennett et al.* [1995]) in the shallow portion of the subduction system, which may influence the overlying topography.

[31] Tomography results are summarized in Figure 7, which shows the shape of the seismically active, high-velocity Ionian slab deepening below the Calabrian Arc. Map views of the tomographic model show that the slab gets narrower as it shallows. The high-velocity body shows its smallest along-strike extent at ~65 km depth (Figure 7), indicating that the slab is continuous only beneath the central part of the arc. At the 65 km depth, the slab extends for ~100 km in a NE-SW direction between the Catanzaro and Messina trough. At this depth, the slab is surrounded by low-velocity anomalies that are particularly evident beneath the Sila massif and the Nebrodi-Etna region in northeastern Sicily. Figures 7d–7f show vertical cross sections obtained from the 3D velocity model of *Neri et al.* [2009] for depths greater than 40 km and from the velocity structure elaborated by *Barberi et al.* [2004] for shallower levels. The vertical section in Figure 7e shows that the slab is continuous beneath southern Calabria and that it changes its attitude from northwesterly inclined to vertical and even to southeasterly overturned. The hinge zone is located beneath the Tyrrhenian Sea, off Calabria. In the slab, the highest concentration of earthquakes (located within ±25 km of the vertical planes) occurs at a depth of about 120–180 km, where the slab thins (Figure 7e).

[32] The southern cross section (Figure 7d) shows a small gap in the high-velocity anomaly at shallow depths beneath the Nebrodi Mts., interrupting the continuity of the slab. A clear gap is also shown in the northern cross section beneath the Sila massif (Figure 7f), where the deeper portion of the slab is totally detached from the shallow portion and a trace of the low-velocity anomaly extends from a depth of 200 km or more to the base of the crust. These images define quite precisely the geometry of the subduction zone, which appears as an extremely necked body enlarging at depth. Its subvertical image suggests an incipient detachment [*Neri et al.*, 2009]. The origin of the low-velocity tomographic anomaly beneath Sila and Nebrodi is disputed and has been interpreted as related either to mantle circulation at the edge of the subduction zone [*Montuori et al.*, 2007], to the presence of melted material [*Chiarabba et al.*, 2008], or to partial harzburgite hydratation and serpentinization [*Caló et al.*, 2009]. Further research is necessary to discriminate between the different interpretations.

5. Discussion

5.1. Topography and Uplift

[33] The topography of mountain belts results from the interplay between tectonics and surface erosion processes. If climate can be assumed as being uniform over the study area, then differential denudation rates depend on erodibility (i.e., rock strength) and tectonics (i.e., faults and rock damage). The above presented evidence shows that the Calabrian Arc is a meaningful site to investigate these processes.

[34] Fission track data indicate that very limited erosion occurred in Calabria [*Thomson*, 1994]. We may then assume that the topography of Calabria mainly results from the Pleistocene uplift event. The height of the MIS 5.5 terraces is consistent with an average uplift rate of 0.8–1 mm/yr [*Westaway*, 1993], which is similar to the uplift rate deduced by the height of the lower Pleistocene marine terrace [*Miyauchi et al.*, 1994]. The overall topography can be then explained by 1 Myr of uplift at a rate of 0.8–1 mm/yr [*Westaway*, 1993].

[35] Our analysis show that the topography of the Calabrian Arc is dominated by the superposition of short-wavelength features, which are likely related to local faulting and regional-scale (≥100 km) wavelength features (Figure 4a). The map of long-wavelength topography (Figure 4a) shows two maxima corresponding to the Nebrodi Mts. and the Sila-Pollino massif, which bound a relatively depressed region corresponding to the area overlying the active Wadati-Benioff zone. The regional-scale topographic bulges (i.e., Nebrodi and Sila-Pollino) extend along strike for more than 100 km. In particular, the long-wavelength bulge of the Nebrodi Mts. gently plunges toward the east and west, locally interrupted by the Tindari and Cefalù faults (Figure 8a). These active faults produce local hanging wall uplift that results from the normal faulting as testified from slip vectors observed over fault planes. This local uplift is clearly recorded by the topography. To the east, the plunge of the Nebrodi bulge is more rapid and influenced by the large-scale fault system of the Messina Straits. In Calabria, the Aspromonte represents a small-wavelength feature, which is very likely modulated by the footwall uplift occurring along the Reggio Calabria and Arno faults [*Monaco and Tortorici*, 2000 and references therein; *Galli and Bosi*, 2002; *Catalano et al.*, 2003]. Moving to the north, the topographic profile remains roughly uniform across Le Serre and then rises toward the high-standing low-relief landscape of the Sila and the Pollino massif, which represents the other long-wavelength topographic bulge. The average differential elevation between the two flanking bulges and the central depressed region depends on the adopted filter, but it ranges between about 500 and 800 m (Figure 8).

[36] The correlation between the topography and marine terraces is usually not straight forward [see also *Bordoni and Valensise*, 1998] as the elevation record of the terraces is usually scattered and affected by their position with respect to the axis of the uplifting structure and because the denu-

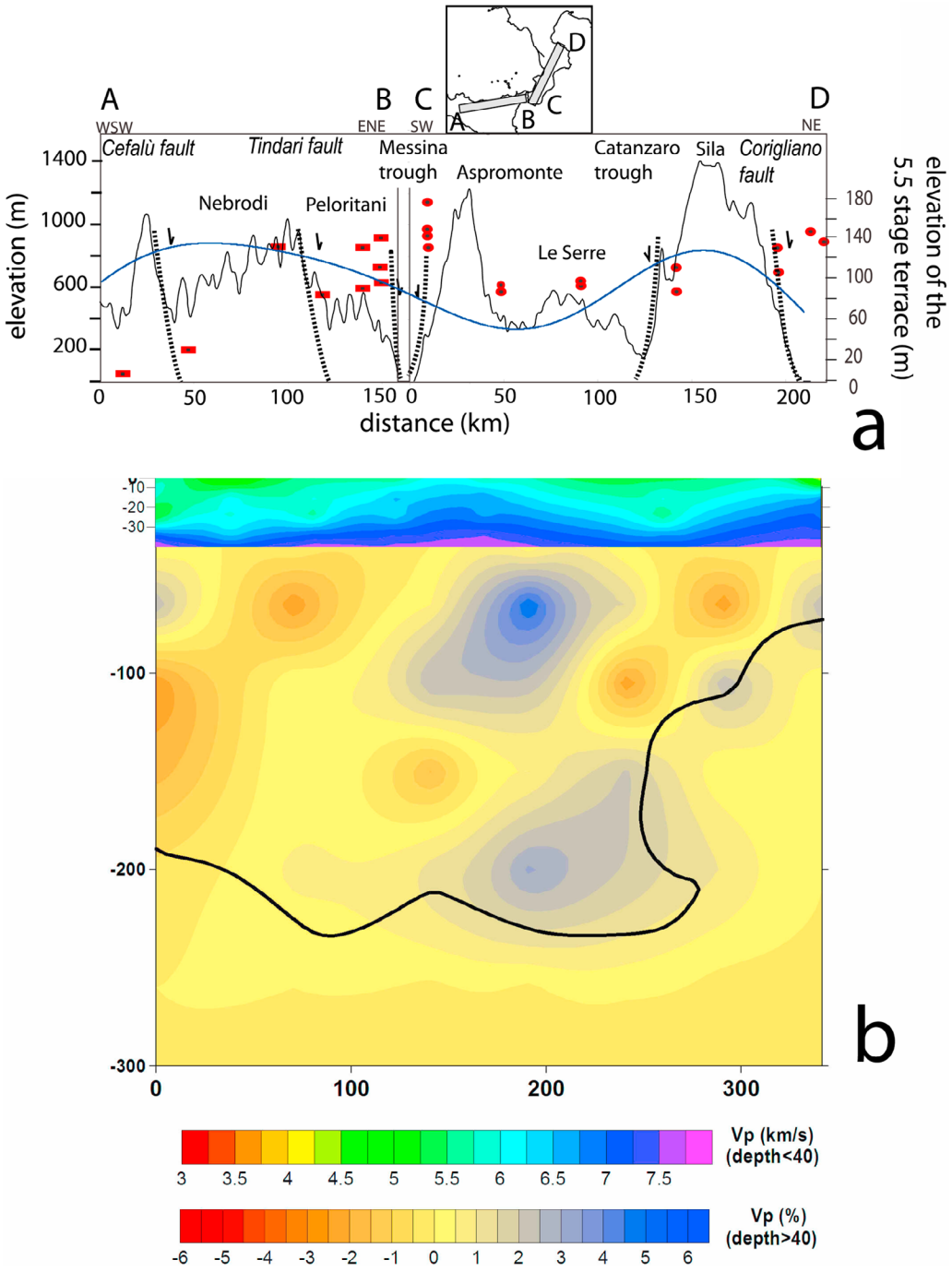

Figure 8. Cross section from Calabria to NE Sicily showing (a) the mean topography, the filter raw topography with cutoff wave lengths of ~100 km (blue curve) and the MIS 5.5 terrace elevation plotted on top of the tomographic model (modified from the model of *Neri et al.* [2009]; black line contours the zone where the spread function values are not larger than 3.25). The comparison shows that the Sila and Nebrodi Mts. positive long-wavelength topography is located on top of (b) low velocity seismic anomalies, whereas the area corresponding with active subduction is characterized by a less-elevated topography and is bounded by Messina and Catanzaro troughs.

dation rate depends strongly on faults and related rock damage. Considering these limitations, we discuss only the general trends observed in Calabria as follows (Figure 8a).

[37] In northern Sicily, topography and uplift produce a large swell with a wavelength on the order of 100–150 km, peaking in the Nebrodi Mts. A reverse trend between topography and uplift is observed in the Messina Straits area, where the highest uplift rate occurs directly on top of a depressed topography (Messina trough) and on the low-altitude range of the Peloritani Mts. This evidence suggests that, in the Messina-Peloritani area, the denudation rate is faster than or similar to the uplift rate and that the tectonic activity of the Messina Straits faults has a significant influence on the local topography. Geodetic measurements show, in fact, that the Messina Straits area is presently extending at a rate of circa 3 mm/yr [*D'Agostino and Selvaggi*, 2004]. Moreover, cosmogenic dating on fluvial sand shows that the erosion rate in the Messina Straits and Peloritani Mts. is anomalously high, that is, on average two to four times higher than that measured in the Sila massif [*Cyr*, 2009; *Olivetti*, 2009]. The local origin of such a fast localized uplift [*Antonioli et al.*, 2006a, 2006b], superimposed on the larger one, can be explained by the presence of the active Messina fault system and by the Mt Etna plumbing system. Topography and terrace elevations show a nice correlation in southern Calabria as well, with an unfaulted progressive descent from Aspromonte to Le Serre well-observed on the whole flight of terraces [*Barrier et al.*, 1986; *Miyauchi et al.*, 1994; *Bordoni and Valensise*, 1998; *Balescu et al.*, 1997; *Ferranti et al.*, 2006]. In contrast, the correlation between topography and terrace elevation cannot be confidently addressed in the Sila massif, where marine terrace data are lacking, especially on the southern flank of the massif. However, from the position of the Rossano terrace, which is located on the hanging wall of a normal fault, we infer that the uplift rate of the Sila massif may be approximately 20–30% higher than that of Le Serre (Figure 5). Further evidence is required to confirm this inference.

5.2. Topography Versus Tomography

[38] Figure 8 presents a synthesis of the comparison between topography, marine surface elevation, and deep evidence presented above for the Calabrian arc. As discussed before, Le Serre is topographically depressed with respect to the adjacent highs of the Sila and Nebrodi Mts. This is even clearer in the long-wavelength topography, where also the Apromonte relief disappears by removing wavelengths shorter than 100 m (Figure 8). Below these two highs, the tomographic model shows low velocity anomalies. In contrast, Le Serre is located on top of the high-velocity anomaly and the seismically active portion of the slab. The correlation between tomography and the long-wavelength topography is also partly supported by the elevation of the MIS 5.5 terrace, indicating that the present day topography is related to the continuous Pleistocene uplift, whose rate is spatially variable. Unfortunately, the lack of data in specific areas and the effect of very high local rates of denudation [*Cyr and Granger*, 2008] prevent a complete comprehension of the distribution of the MIS 5.5 terraces and a correlation more robust than that shown in Figure 8 (see section 5.1). In particular, the main problematic issues about this correlation concern the Messina trough area and the nearby Aspromonte Mts. A comparison with tomographic data suggests that this area is positioned on top of the southern edge of the high-velocity anomaly. In this view, the activity of the Messina fault responsible, on 28 December 1908, of one of the largest and most destructive earthquakes in the central Mediterranean (M_w = 7.2) and subjected to an ongoing extensional rate of circa 3 mm/yr (Figure 1; *D'Agostino and Selvaggi* [2004]) could represent the shallow expression of mantle deformation around the southern side of the subducting slab. The finding that the Aspromonte Mt. relief is smoothed out by large-wavelength filters suggests that at least part of this relief is elastically supported by the crust in this area of rapid deformation. Further analyses and tomographic images at a resolution higher than those used in this paper are necessary to support this hypothesis.

6. A Model for Calabria Deformation

[39] The main points on the Calabria deformation can be summarized as follows. 1. A general consensus exists in considering that the topography of the Calabrian belt is the result of a recent uplift of an old, poorly-eroded landscape [*Thomson*, 1994] still preserved on top of Sila, Le Serre, and Aspromonte [*Dumas et al.*, 1982; 1988; *Barrier et al.*, 1986; *Miyauchi et al.*, 1994; *Dramis et al.*, 1990; *Molin et al.*, 2004]. In addition, the topography of Calabria shows large-wavelength undulations with relative large-wavelength highs positioned to the north (Sila massif) and southwest (Nebrodi) of Le Serre massif.

[40] 2. A general consensus exists in considering that the uplift rate deduced from MIS 5.5 terraces elevation is in the order of 0.8–1 mm/yr [*Westaway*, 1993] and that the onset of uplift is in the lower Pleistocene [*Miyauchi et al.*, 1994]. In addition to that, the record of the uplift rate, although incomplete, shows along strike variation, increasing by about 30% to the north and southwest of Le Serre, at least during the last 125 ka.

[41] 3. Several tomographic studies and the Wadati-Benioff zone distribution indicate that the slab is narrow. The regional tomography analysis [*Neri et al.*, 2009] shows that the slab is presently continuous only beneath Le Serre. Tectonic reconstructions indicate that the present day slab geometry is related to lateral slab tearing and necking episodes in early Pleistocene time. Hence, uplift likely initiated when the active subduction became as narrow as it is at present.

[42] 4. It is generally recognized that the Calabrian arc is under extension at least from the lower Pleistocene onward, but the orientation of the extensional axis varies along strike. The lateral slab boundary is marked by two systems of normal faults (i.e., Messina and Catanzaro areas faults) located to the south and north of the Wadati-Benioff zone, respectively, and striking at a high angle with respect to the axis of the belt. The strain field also varies along the arc. At Le Serre, on top of the active portion of the Wadati-Benioff zone, normal faults strike parallel to the chain axis and are characterized by a

normal displacement mainly perpendicular to the slab strike (i.e., NW-SE). To the north and south of this area, near the top of the slab edge, the most recent direction of extension turns to the ENE-WSW direction.

[43] 5. Mount Etna volcanism is positioned on top of a highly uplifted and still uplifting region indicating, together with Etna's volcanism itself, upwelling on the slab's edge.

[44] Four different classes of models have been proposed to explain uplift and deformation process in Calabria: 1. uncoupling along a weak subduction fault [*Giunchi et al.*, 1996]; 2. active compression and/or under plating; 3. unloading due to slab break off [*Westaway*, 1993; *Wortel and Spakman*, 2000; *Buiter et al.*, 2002] or to lithosphere mantle removal on top of subducting slab [*Gvirtzman and Nur*, 1999]; and 4. dynamic topography related to circulation around a narrow, retreating, subducting slab [*Dvorkin et al.*, 1993; *Gvirtzman and Nur*, 1999; *Faccenna et al.*, 2004, 2005].

[45] Comments on each model are proposed below.

[46] 1. The weak fault model is appealing, but it does not explain both why uplift accelerated in early Pleistocene time and why it varied along strike.

[47] 2. Uplift could be related to crustal thickening and underplating. This model could apply to the northern Calabria (Pollino) Southern Apennines [*Ferranti et al.*, 2009; *Caputo et al.*, 2010] but, south of Pollino, compression was active until the Pliocene and then vanished [*Roveri et al.*, 1992], ruling out the possible support derived from active convergence. The fast subduction regime indeed responsible for the growth of the Neogene accretionary wedge [*Minelli and Faccenna*, 2010], slowed down from the Middle Pleistocene onward to rate of only a few mm/yr (5 mm/yr [*D'Agostino and Selvaggi*, 2004; *Devoti et al.*, 2008]). Shortening is presently accommodated within the outer arc.

[48] 3. Slab break off [*Westaway*, 1993; *Wortel and Spakman*, 2000] and mantle removal [*Gvirtzman and Nur*, 1999] represents the most commonly accepted models for Calabria. The hypothesis is that rebound after unloading could have indeed produced uplift of the upper plate. However, the time scale of this process is rheology dependent and the rebound can be hindered by the viscous component of the lithosphere, producing viscous necking and deblobbing, rather than break off. In addition, slab-mantle viscous coupling is expected to produce subsidence rather then uplift during the fall of the detached portion of the slab [*Marotta et al.*, 1998; *Gerya et al.*, 2004]. Our analysis supports this general model, as the lack of a deep-subducting structure is marked by larger uplift [*Westaway*, 1993; *Wortel and Spakman*, 2000], whereas available data cannot directly test the idea of lithosphere mantle thinning. However, the fact that uplift and elevation are also registered beneath Le Serre, where slab is continuous and active, suggests that other mechanisms in addition to the elastic rebound could also operate in the region. In addition, the general uplift trend, lasting for about 1 Ma, cannot be easily interpreted as an isostatic rebound signal, because such a signal should have operated at a time scale in the order of 10^4 years.

[49] 4. The last model suggests that the deformation history of Calabria and the Etna's volcanism could have been originated dynamically by the action of a complex 3D mantle flow around the slab edge [*Dvorkin et al.*, 1993; *Gvirtzman and Nur*, 1999; *Trua et al.*, 2003; *Civello and Margheriti*, 2004; *Faccenna et al.*; 2004, 2005]. Toroidal flow (i.e., a horizontal rotational vortex-like component of mantle motion) is in fact expected on the sides of a retreating or steepening slab and has been tested by analytical [*Dvorkin et al.*, 1993; *Royden and Husson*, 2006], laboratory [*Kincaid and Griffiths*, 2003; *Funiciello et al.*, 2003, 2006; *Schellart*, 2004; *Faccenna et al.*, 2007], and numerical solutions [*Piromallo et al.*, 2006; *Stegman et al.*, 2006; *Di Giuseppe et al.*, 2008]. Figure 9 illustrates one of the models extracted from the numerical simulation by *Piromallo et al.* [2006] (CitcomS finite element code, see *Moresi and Solomatov* [1998] and *Zhong et al.* [2000]). This model shows the instantaneous mantle flow generated by the subduction of an isolated slab adapted to the case of Calabria [*Piromallo and Morelli*, 2003]. Imposing this slab geometry, resting horizontally at the 660 km discontinuity (Figure 9), the toroidal component dominates over the poloidal component (upwelling and downwelling). *Piromallo et al.* [2006] and *Funiciello et al.* [2006], in fact, show that toroidal motion is mostly excited during retrograde slab motion, or by its steepening as mantle material beneath the slab is displaced toward its front, flowing laterally around the edges and producing two symmetrical vortex-like structures (Figure 9) whose maximum velocities scale with trench velocity [*Funiciello et al.*, 2006]. The peculiarity of mantle circulation during this stage is indicated by the presence of pronounced upper mantle upwelling at the slab edges. This feature results from the continuous interplay between poloidal and toroidal fluxes and is expected to produce uplift of the over-riding plate and also volcanism induced by decompression melting.

[50] The application of modeling results to the case of Calabria is limited by the inherent simplicity of the adopted setting and by the incomplete record of our data set. For example, the 20–30% variation topography and uplift rate along the strike of the arc reconstructed here are complicated by the superimposed small-wavelength tectonic signals. Being aware of these complications, we consider the latter model as the most appropriate one to explain the pattern of deformation in Calabria, for the following reasons.

[51] *Differential uplift and topography*. Superimposing the mantle velocity field, as deduced from numerical models, on the tomographic image of Calabria (layer at 150 km depth; Figure 10 from *Piromallo and Morelli* [2003]) shows the area where we would expect to have mantle upwelling and, therefore, uplift corresponding to the Sila-Pollino and Nebrodi-Peloritani swellings. Whereas the amount of predicted uplift and decompression melting is a function of the viscosity structure of the mantle [*Piromallo et al.*, 2006], the location of the focused return flow is robust irrespective of the adopted boundary condition or rheological structure. In this view, toroidal flow could be responsible for 20–30% of the extra uplift observed at slab edge.

[52] *Timing and rate of uplift*. Toroidal flow is expected to operate as long as the subduction zone operates. This model is able to explain the long-term, apparently continuous,

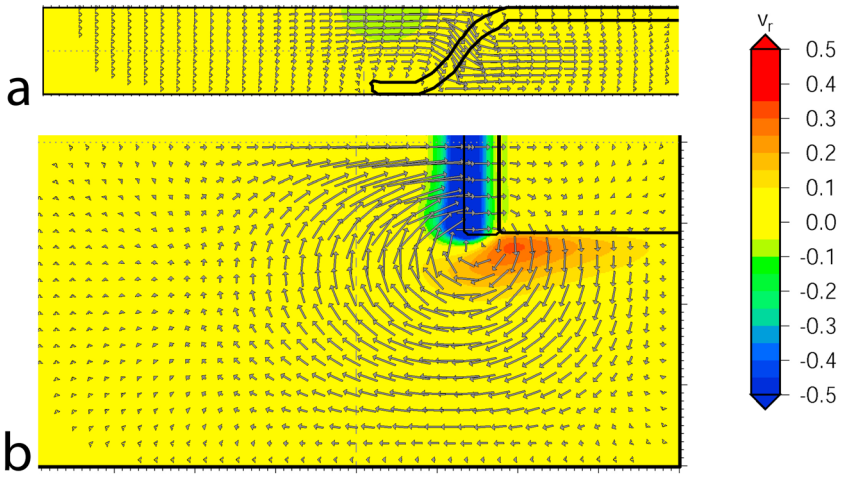

Figure 9. Instantaneous numerical solution of a 3D subduction-induced flow from a simulation by *Piromallo et al.* [2006]. (a) Cross section and (b) plan view at 150 km depth. (right) Colors indicate the vertical component of mantle flow, with red indicating upwelling and green-blue indicating downwelling. Models are performed with finite element code CitcomS (see *Moresi and Solomatov* [1998] and *Zhong et al.* [2000] for details), solving the conservation equations for mass, momentum, and energy in the Boussinesq approximation, assuming that the mantle is an incompressible viscous medium (see *Zhong et al.* [2000] for details). The slab shape is set similar to the actual Calabrian one inferred from tomographic images (Figure 9a). The numerical domain is 7.4 × 7.4 × 1 in the *x*, *y*, and *z* directions respectively, representing a box that is 4900 km wide and 660 km deep (one nondimensional length unit scales to 660 km). The slab is a Newtonian, 100 km thick, constant density body attached to one side of the box (simulating Africa). For details and parameters see *Piromallo et al.* [2006]. Note that vertical upwelling is located right at the slab edges and is connected with the vertical part of the toroidal flow component.

uplifting over a time scale (10^6 years) far longer than that expected from the isostatic readjustment (10^3–10^4 years) related to any form of removal of a deep load. The timing of initiation of vigorous uplift fits with the Lower Pleistocene phase of slab necking, suggesting indeed that slab narrowing is responsible for increases in toroidal motion. We speculate that this may have generated by steepening of the slab, as proposed by *Gvirtzman and Nur* [2001].

[53] *Volcanism*. Upwelling of the mantle predicted by our model in the center of the vortex is expected to produce decompression melting. The expected upwelling aligns with the position of Mt Etna. Although the location of Mt. Etna is clearly controlled by the presence of crustal structure we speculate that its deep root can be due to the presence of toroidal flow at slab edge generating decompression melting. Low-velocity anomalies at the southern edge of the Calabrian slab are in general agreement with this analysis [*Piromallo and Morelli*, 2003; *Montuori et al.*, 2007], even if the possible role of fluid release from the subducting slab cannot be ruled out [*Caló et al.*, 2009].

[54] *Gravity anomalies*. Gravity profiles along Calabria, interpreted on the grounds of theoretical modeling, reveal that transitions from continuous to detached subduction mode occur beneath the Messina Straits and the Sila Massif [*Marotta et al.*, 2007], in agreement with the tomographic model shown here. At a larger scale, gravity anomaly analysis also indicates that the area is out of isostatic equilibrium [*Cella et al.*, 2006]. More important, frequency analysis of the free-air gravity anomaly and topography performed along the Apennines [*D'Agostino and McKenzie*, 1999; *D'Agostino et al.*, 2001], where anomalies show positive values as high as in Calabria, indicate that the long-wavelength topography component (>100 km) is compensated at mantle depths and that the topography is sustained by mantle upwelling. A more accurate analysis of the admittance is required to validate the possible presence of a dynamic signal or the possible role of crustal structure to explain the different topographic signal.

[55] *Mantle anisotropy*. The planform of the expected mantle flow calculated in the experiment can also be qualitatively compared with the *SKS* splitting data (a proxy for upper mantle flow) compiled by *Civello and Margheriti* [2004] (Figure 10). The correspondence between the modeling of mantle velocity field and the seismological dataset is quite remarkable in western Sicily, where *SKS* fast directions strike N–S, perpendicular to the axis of the belt, and then turn abruptly to the E–W direction in the Tyrrhenian region. However, the model fails to reproduce the orientation of the *SKS* splitting directions in the southern Apennines, at high angle (parallel to the belt) to the expected flow lines. *Faccenna et al.* [2005] explain this pattern as likely related to the different ages of slab windows

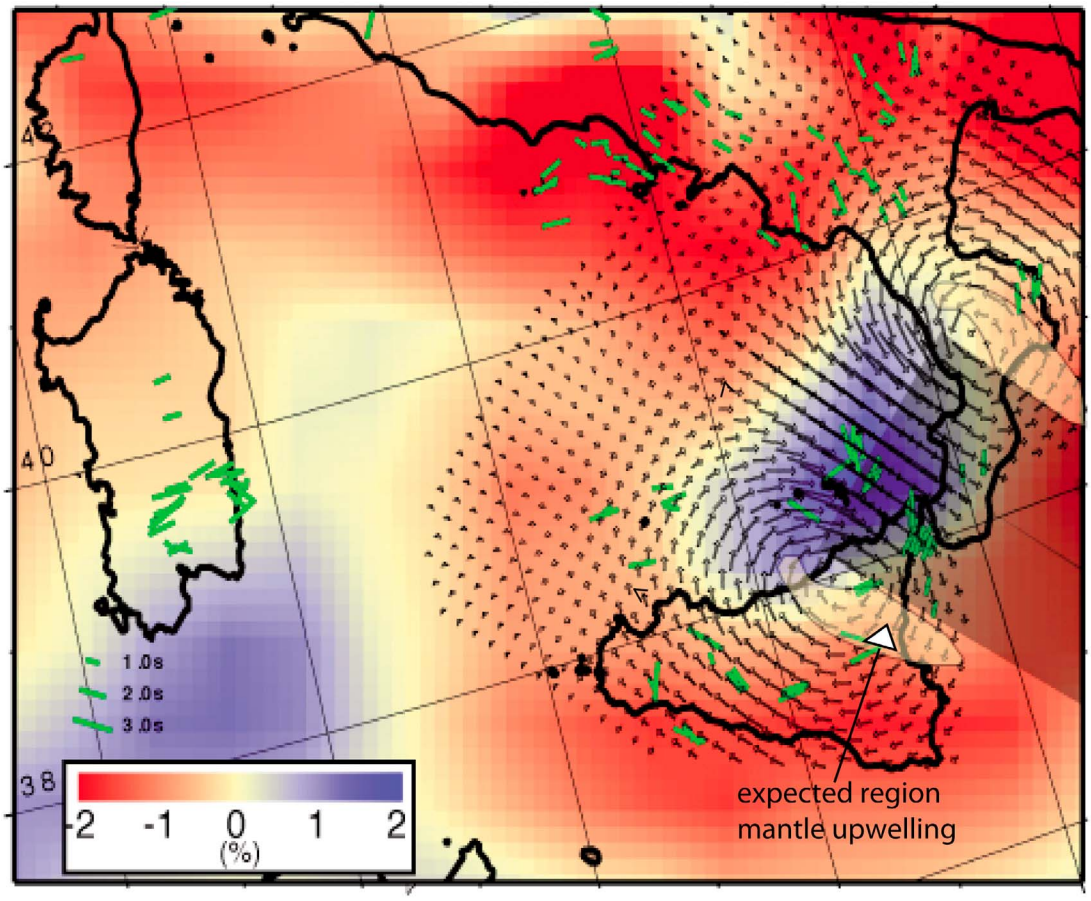

Figure 10. Superposition of the model run as in Figure 9a over a horizontal section 150 km deep of the *P* wave tomographic model by *Piromallo and Morelli* [2003] with colors indicating percentage deviation of *P* velocities from mantle reference velocities. Note the match between the expected uplifting area from mantle upwelling (pink areas at slab edges), the long-wavelength topography, and Mount Etna volcanism (see Figure 4a). Reported in green are the results from *SKS* splitting data after *Civello and Margheriti* [2004].

bordering the Calabrian subducting lithosphere. The slab window in western Sicily is older than that in the southern Apennines (Figure 2), where the total accumulated strain in the mantle may have been too limited to be seismologically detected by anisotropy studies.

[56] *Deformation pattern*. The velocity field generated by the toroidal flow is expected to generate, at surface, complex tectonic signals due to the lateral velocity gradient that could result in a strike-slip component of deformation [*Funiciello et al.*, 2006]. In agreement with the analysis of *Goes et al.* [2004], we speculate that the change in the strain field registered by the slip on main faults could result from the plate reorganization and related deep mantle flow on the side of the narrow slab. More detailed experiments are required to better simulate the expected deformation field at slab edges.

[57] The model proposed here contains ingredients of previous models. It confirms, in fact, that uplift is located in correspondence of low-velocity anomalies [*Wortel and Spakman*, 2000] and that mantle circulation around a narrow slab can produce a complex 3D geometry [*Gvirtzman and Nur*, 1999]. The presence of the relatively depressed feature over the active subducting portion of the slab (i.e., Le Serre) also supports the current idea that mantle flow dragged down by the subducting slab produces a (relatively) negative dynamic topography, well-expressed here in the back arc region as well (Marsili basin).

[58] We propose that the reduction and necking of the slab in the lower Pleistocene produced a sudden decrease in the mass anomaly inducing an overall uplift of the upper plate (Figure 11). We also propose that the resulting toroidal flow at slab edge could have been responsible for the large wavelength positive features occurring at the edge of the Wadati-Benioff zone in Calabria. This process is able to reconcile the long-term, out-of-isostasy uplift on the order of about some hundreds of meters and help to explain the deep, still enigmatic, source of the conspicuous volcanism of Mt Etna (Figure 11). To validate this model we need

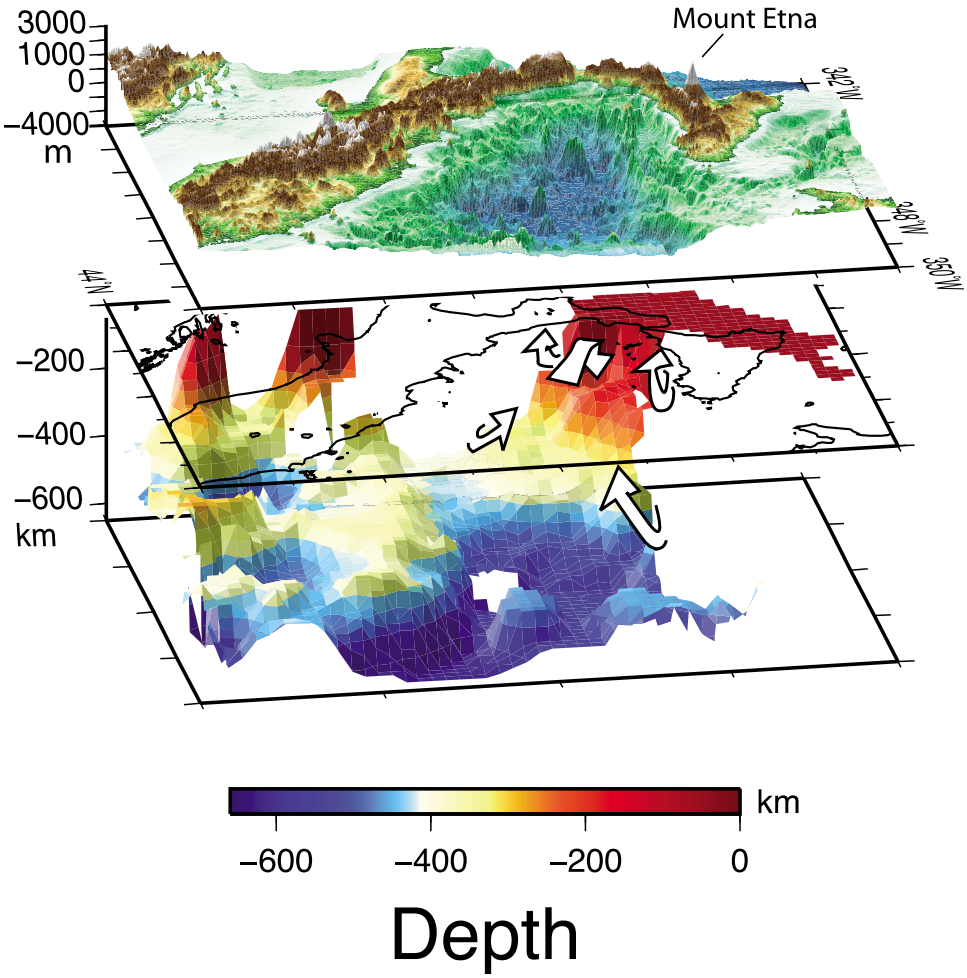

Figure 11. 3D view showing the topography of the Southern Tyrrhenian region positioned on top of the isosurface enclosing a volume characterized by *P* wave velocity anomalies larger than 0.8% relative to mantle average velocities (from *Piromallo and Morelli*, 2003). Colors indicate depth. Arrows indicate the pattern of mantle flow expected on the sides and on top of the narrow subducting Calabrian slab.

further analyses such as the attitude of the marine terraces and their bearing with topography, for example on the southern side of the southern Sila massif, where few data are available. It would be also important to better define the long-term rate of uplift and to confirm that the onset of uplift occurred once the slab reduced its width to the present day length. Similarly, the deep structure of the lithosphere is still poorly constrained and high-resolution images would help to understand if the differential topography is sustained by some lateral variations in the crustal and thermal structure. In addition, more sophisticated seismological analyses are required to constrain the nature (thermal versus compositional) of the low-velocity tomographic anomalies positioned beneath the topographic swelling in Calabria.

7. Conclusions

[59] The Calabrian arc represents a key site to analyze the deformation and volcanism around a narrow, subducting slab. We analyzed the deformation of the curved belt, including an analysis of topography at different wavelengths, the record of the uplift of recent, well-marked marine terraces, and the strain field recorded by slip along the main recently active faults. We compared our result with a recent, high-resolution tomography study that highlights the structure of the slab.

[60] Our results emphasize the importance of the 3D analysis over the narrow subducting slab. In particular, we find that in correspondence with the active portion of the subducting slab (i.e. in the center of the arc), topography and uplift are substantially lower than those at the slab edges. The slip data along the main faults also show a change in the strain field moving from the center of the arc, where slip is normal to the subduction zone, and to the wings, where the slip pattern is more complicated. Long wavelengths and uplift at the slab edges reveal the presence of a non-compensated large-scale swelling, larger than >100 km, possibly positioned on top of the low-velocity anomaly in

the upper mantle. Supported by the result of numerical models, we propose that the deformation (i.e., uplift and faulting) at the top of the Calabrian slab edges is sustained dynamically by toroidal flow in the mantle, excited at the edges by the retreat and steepening of the narrow Calabrian slab. This process provides favorable conditions for decompression melting, feeding Mt Etna volcano.

[61] Our results demonstrate the drastic influence of the mantle processes on the Earth's surface changes (e.g., topography, shallow tectonics, and volcanism) and the importance of 3D analysis to unravel the complex surface deformations occurring on top of an active subduction zone.

[62] **Acknowledgments.** This project was funded by MIUR ("Recent evolution of the Calabrian subduction zone: geological, geophysical and geochemical constraints" led by C.F.), under the support of the TOPOMED project (ESF) and of S1 Protezione Civile, and carried out by the Roma TRE team, led by Renato Funiciello. It also benefited from the discussion and collaboration with the Calabrian Arc project team funded by the NSF (EAR 06-07687) and led by M. Steckler. T.W. Becker contributed substantially to the numerical solution. G. Neri and D. Presti contributed to the seismological solution. Benjamin Guillaume provided Figures 2 and 11 and N. D'Agostino provided Figure 1. We also thank for interesting discussions L. Civetta, M. D'Antonio, N. D'Agostino, F. Dramis, L. Ferranti, G. Giunta, P. Lucente, L. Margheriti, M. Mattei, F. Pazzaglia, N. Seeber, M. Steckler, W. Spakman, R. Wortel, and others. We wish to thank the Editor and reviewers (Anonymous and Laurent Husson) for their suggestions and their comments.

References

Anderson, H., and J. Jackson (1987), Active tectonics of the Adriatic Region, *Geophys. J. R. Astronom. Soc.*, *91*, 937–983.

Antonioli, F., L. Ferranti, K. Lambeck, S. Kershaw, V. Verrubbi, and G. Dai Pra (2006a), Late Pleistocene to Holocene record of changing uplift rates in southern Calabria and northeastern Sicily (southern Italy, central Mediterranean Sea), *Tectonophysics*, *422*, 23–40.

Antonioli, F., S. Kershaw, P. Renda, D. Rust, G. Belluomini, U. Radtke, and S. Silenzi (2006b), Elevation of the last interglacial highstand in Sicily (Italy): A benchmark of coastal tectonics, *Quat. Int.*, *145–146*, 3–18, doi:10.1016/j.quaint.2005.07.002.

Antonioli, F., et al. (2009), Holocene relative sea level changes and vertical movements along the Italian and Istrian coastlines, *Quat. Int.*, *206*, 102–133.

Argnani, A., S. Cornini, L. Torelli, and N. Zitellini (1987), Diachronous foredeep-system in the Neogene-Quaternary of the Strait of Sicily, *Mem. Soc. Geol. It.*, *38*, 407–417.

Balescu, S., B. Dumas, P. Guermy, M. Lamothe, R. Lhenaff, and J. Raffy (1997), Thermoluminescence dating test of Pleistocene sediments from uplifted shorelines along the southwest coastline of the Calabrian peninsula (southern Italy), *Palaeogeogr. Palaeoclimatol. Palaeoecol.*, *130*, 25–41.

Barberi, G., M. T. Cosentino, A. Gervasi, I. Guerra, G. Neri, and B. Orecchio (2004), Crustal seismic tomography in the Calabrian Arc region, south Italy, *Phys. Earth Planet. Int.*, *147*, 297–314.

Bardají, T., J. L. Goy, C. Zazo, C. Hillaire-Marcel, C. J. Dabrio, A. Cabero, B. Ghaleb, P.G. Silva, and J. Lario (2009), Sea level and climate changes during OIS 5e in the Western Mediterranean, *Geomorphology*, *104*, 22–37.

Barrier, P., I. Di Geronimo, and G. Lanzafame (1986), I rapporti tra tettonica e sedimentazione nell'evoluzione recente dell'Aspromonte Occidentale (Calabria), *Riv. It. Paleont. Strat.*, *91*, 537–556.

Billen, M. I., M. Gurnis, and M. Simons (2003), Multiscale dynamic models of the Tonga-Kermadec subduction zone, *Geophys. J. Int.*, *153*, 359–388.

Billi, A., G. Barberi, C. Faccenna, G. Neri, F. Pepe, and A. Sulli (2006), Tectonics and seismicity of the Tindari Fault System, southern Italy: Crustal deformations at the transition between ongoing contractional and extensional domains located above the edge of a subducting slab, *Tectonics*, *25*, TC2006, doi:10.1029/2004TC001763.

Billi, A., D. Presti, C. Faccenna, G. Neri, and B. Orecchio (2007), Seismotectonics of the Nubia plate compressive margin in the south-Tyrrhenian region, Italy: Clues for subduction inception, *J. Geophys. Res.*, *112*, B08302, doi:10.1029/2006JB004837.

Billi, A., D. Presti, B. Orecchio, C. Faccenna, and G. Neri (2010), Incipient extension along the active convergent margin of Nubia in Sicily, Italy: Cefalù-Etna seismic zone, *Tectonics*, *29*, TC4026, doi:10.1029/2009TC002559.

Bordoni, P., and G. Valensise (1998), Deformation of the 125 ka marine terrace in Italy: Tectonic implications, in *Coastal Tectonics*, edited by I. S. Stewart and C. Vita-Finzi, *Geol. Soc. Spec.Publ.*, 146, 71–110.

Bousquet, J.C., P. Carveni, G. Lanzafame, H. Philip, and L. Tortorici (1980), La distension pleistocene sur le bord oriental du detroit de Messina: Analogies entre les resultats microtectoniques et le mecanisme au foyer du sisme de 1908, *Bull. Soc. Geol. France*, *22*, 327–336.

Buiter, S. J. H., R. Govers, and M. J. R. Wortel (2002), Two-dimensional simulations of surface deformation caused by slab detachment, *Tectonophysics*, *354*, 195–210.

Burrus, J. (1984), Contribution to a geodynamic synthesis of the Provençal basin (northwestern Mediterranean), *Mar. Geol.*, *55*, 247–269.

Caló, M., C. Dorbath, D. Luzio, S. G. Rotolo, and G. D'Anna (2009), Local earthquake tomography in the southern Tyrrhenian region of Italy: Geophysical and petrological inferences on the subducting lithosphere, in *Subduction Zone Geodynamics*, edited by S. Lallemand and F. Funiciello, pp. 85–99, Springer, New York.

Caputo, R., M. Bianca, and R. D'Onofrio (2010), Ionian marine terraces of southern Italy: Insights into the Quaternary tectonic evolution of the area, *Tectonics*, *29*, TC4005, doi:10.1029/2009TC002625.

Carminati, E., R. Wortel, W. Spakman, and R. Sabadini (1998), The role of slab-detachment processes in the opening of the western-central Mediterranean basins: Some geological and geophysical evidence, *Earth Planet. Sci. Lett.*, *160*, 651–665, doi:10.1016/S0012-821X(98)00118-6.

Casero, P., and F. Roure (1994), Neogene deformations at the Sicilian-North African Plate boundary, in *Peri Tethyan Platforms*, edited by F. Roure, pp. 27–50, Editions Technip, Paris.

Catalano, R., C. Doglioni, and S. Merlini (2001), On the Mesozoic Ionian basin, *Geophys. J. Int.*, *144*, 49–64.

Catalano, S., G. De Guidi, C. Monaco, G. Tortorici, and L. Tortorici (2003), Long-term behavior of the late Quaternary normal faults in the Straits of Messina area (Calabrian arc): Structural and morphological constraints, *Quat. Int.*, *101–102*, 81–91.

Catalano, S., G. De Guidi, G. Romagnoli, S. Torrisi, G. Tortorici, and L. Tortorici (2008), The migration of plate boundaries in SE Sicily: Influence on the large-scale kinematic model of the African promontory in southern Italy, *Tectonophysics*, *449*, 41–62 doi:10.1016/j.tecto.2007.12.003.

Cella, F., S. De Lorenzo, M. Fedi, M. Loddo, F. Mongelli, A. Rapolla, and G. Zito (2006), Temperature and density of the Tyrrhenian lithosphere and slab and new interpretation of gravity field in the Tyrrhenian Basin, *Tectonophysics*, *412*, 27–47, doi:10.1016/j.tecto.2005.08.025.

Cello, G., I. Guerra, L. Tortorici, E. Turco, and R. Scarpa (1982), Geometry of the neotectonic stress field in southern Italy: Geological and seismological evidence, *J. Struct. Geol.*, *4*, 385–393.

Chapell, J., A. Omura, T. Esat, M. McCullogh, J. Pandolfi, Y. Ota, and B. Pillans (1996), Reconciliation of late Quaternary sea levels derived from coral terraces at Huon Peninsula with deep sea oxygen isotope records, *Earth Planet. Sci. Lett.*, *141*, 227–236.

Cherchi, A., and L. Montandert (1982), Oligo-Miocene rift of Sardinia and the early history of the Western Mediterranean basin, *Nature*, *298*, 736–739.

Chiarabba, C., L. Jovane, and R. Di Stefano (2005), A new view of Italian seismicity using 20 years of instrumental recordings, *Tectonophysics*, *395*, 251–268.

Chiarabba, C., P. De Gori, and F. Speranza (2008), The southern Tyrrhenian subduction zone: Deep geometry, magmatism, and Plio-Pleistocene evolution, *Earth Planet. Sci. Lett.*, *268*, 408–423; doi:10.1016/j.epsl.2008.01.036.

Ciaranfi, N., F. Ghisetti, M. Guida, G. Iaccarino, P. Pieri, L. Rapisardi, G. Ricchetti, M. Torre, L Tortorici, and L Vezzani (1983), Carta neotettonica dell'Italia meridionale, *Prog. Fin. Geod.*, *515*, 62 pp., Cons. Naz. Ric., Bari, Italy.

Cifelli, F., F. Rossetti, and M. Mattei (2007a), The architecture of brittle postorogenic extension: Results from an integrated structural and paleomagnetic study in North Calabria (Southern Italy), *Geol. Soc. Am. Bull.*, *119*, 221–239; doi:10.1130/B25900.1.

Cifelli, F., M. Mattei, and F. Rossetti (2007b), Tectonic evolution of arcuate mountain belts on top of a retreating subduction slab: The example of the Calabrian Arc, *J. Geophys. Res.*, *112*, B09101, doi:10.1029/2006JB004848.

Civello, S., and L. Margheriti (2004), Toroidal mantle flow around the Calabrian slab (Italy) from SKS splitting, *Geophys. Res. Lett.*, *31*, L10601, doi:10.1029/2004GL019607.

Cosentino, D., and E. Gliozzi (1989), Sulle velocità di sollevamento di depositi Eutirreniani dell' Italia Meridionale e della Sicilia, *Mem. Soc. Geol. It.*, *41*, 653–665.

Cyr, A. J. (2009), Quantifying relationships between erosion and uplift in tectonically active landscapes, Italy, using cosmogenic nuclides and channel morphometry, Ph.D. thesis, 209 pp., Purdue University, West Lafayette, Indiana.

Cyr, A. J., and D. E. Granger (2008), Dynamic equilibrium among erosion, river incision, and coastal uplift in the northern Apennines, Italy, *Geology*, *36*, 103–106.

D'Agostino, N., and D. McKenzie (1999), Convective support of long-wavelength topography in the Apennines, *Terra Nova*, *11*, 234–238.

D'Agostino, N., and G. Selvaggi (2004), Crustal motion along the Eurasia-Nubia plate boundary in the Calabrian Arc and Sicily and active extension in the Messina Straits from GPS measurements, *J. Geophys. Res.*, *109*, B11402, doi:10.1029/2004JB002998.

D'Agostino, N., J. A. Jackson, F. Dramis, and R. Funiciello (2001), Interactions between mantle upwelling, drainage evolution, and active normal faulting: An example from the central Apennines (Italy), *Geophys. J. Int.*, *147*, 475–497.

De Franco, R., R. Govers, and R. Wortel (2008), Dynamics of continental collision: Influence of the plate contact, *Geophys. J. Int.*, *174*, 1101–1120, doi:10.1111/j.1365-246X.2008.03857.x.

Devoti, R., F. Riguzzi, M. Cuffaro, and C. Doglioni (2008), New GPS constraints on the kinematics of the Apennines subduction, *Earth Planet. Sci. Lett.*, *273*, 163–174.

Di Giuseppe, E., J. van Hunen, F. Funiciello, C. Faccenna, and D. Giardini (2008), Slab stiffness control of trench motion: Insights from numerical models, *Geochem. Geophys. Geosyst.*, *9*, Q02014, doi:10.1029/2007GC001776.

Doglioni, C., S. Merlini, and G. Cantarella (1999), Foredeep geometries at the front of the Apennines in the Ionian sea (central Mediterranean), *Earth Planet. Sci. Lett.*, *168*, 243–254, doi:10.1016/S0012-821X(99)00059-X.

Doglioni, C., F. Innocenti, and G. Mariotti (2001), Why Mt Etna?, *Terra Nova*, *13*, 25–31.

Doglioni, C., E. Carminati, M. Cuffaro, and D. Scrocca (2007), Subduction kinematics and dynamic constraints, *Earth Sci. Rev.*, *83*, 125–175, doi:10.1016/j.earscirev.2007.04.001.

Dramis, F., B. Gentili, and G. Pambianchi (1990), Geomorphological scheme of the River Trionto basin, in *Symposium on Geomorphology of Active Tectonic Area, Excursion Guidebook*, pp. 63–66, Int. Geogr. Union, Com. Meas. Theory Appl. Geomorphol., and Cons. Naz. Ric., Cosenza, Italy.

Dumas, B., P. Gueremy, R. Lhenaff, and J. Raffy (1982), Le soulevement quaternaire de la Calabrie meridionale, *Rev. Géol. Dynam. Géogr. Phys.*, *23*, 27–40.

Dumas, B., P. Gueremy, and J. Raffy (2005), Evidence for sea-level oscillations by the "characteristic thickness" of marine deposits from raised terraces of Southern Calabria (Italy), *Quat. Sci. Rev.*, *24*, 2120–2136.

Dumas, B., P. Gueremy, P. J. Hearty, R. Lhenaff, and J. Raffy (1988), Morphometric analysis and amino acid geochronology of uplifted shorelines in a tectonic region near Reggio Calabria, South Italy, *Palaeogeogr. Palaeoclimatol. Palaeoecol.*, *68*, 273–289.

Dvorkin, J., A. Nur, G. Mavko, and A. Z. Ben (1993), Narrow subducting slabs and the origin of backarc basins, *Tectonophysics*, *227*, 63–79.

Faccenna, C., C. Piromallo, A. Crespo-Blanc, L. Jolivet, and F. Rossetti (2004), Lateral slab deformation and the origin of the Western Mediterranean arcs, *Tectonics*, *23*, TC1012, doi:10.1029/2002TC001488.

Faccenna, C., L. Civetta, M. D'Antonio, F. Funiciello, L. Margheriti, and C. Piromallo (2005), Constraints on mantle circulation around the deforming Calabrian slab, *Geophys. Res. Lett.*, *32*, L06311, doi:10.1029/2004GL021874.

Faccenna, C., A. Heuret, F. Funiciello, S. Lallemand, and T. W. Becker (2007), Predicting trench and plate motion from the dynamics of a strong slab, *Earth Planet. Sci. Lett.*, *257*, 29–36.

Ferranti, L., et al. (2006), Markers of the last interglacial sea level highstand along the coast of Italy: Tectonic implications, *Quat. Int.*, *145–146*, 30–54, doi:10.1016/j.quaint.2005.07.009.

Ferranti, L., E. Santoro, M. E. Mazzella, C. Monaco, and D. Morelli (2009), Active transpression in the northern Calabria Apennines, southern Italy, *Tectonophysics*, *476*, 226–251, doi:10.1016/j.tecto.2008.11.010.

Funiciello, F., C. Faccenna, D. Giardini, and K. Regenauer-Lieb (2003), Dynamics of retreating slabs (part 2): Insights from 3D laboratory experiments, *J. Geophys. Res.*, *108*(B4), 2207, doi:10.1029/2001JB000896.

Funiciello, F., M. Moroni, C. Piromallo, C. Faccenna, C. Cenedese, and H.A. Bui (2006), Mapping mantle flow during retreating subduction: Laboratory models analyzed by feature tracking, *J. Geophys. Res.*, *111*, B03402, doi:10.1029/2005JB003792.

Galli, P., and V. Bosi (2002), Paleoseismology along the Cittanova fault: Implications for seismotectonics and earthquake recurrence in Calabria (southern Italy), *J. Geophys. Res.*, *107*(B3), 2044, doi:10.1029/2001JB000234.

Galli, P., and V. Bosi (2003), Catastrophic 1638 earthquakes in Calabria (southern Italy): New insights from paleoseismological investigation, *J. Geophys. Res.*, *108*(B1), 2004, doi:10.1029/2001JB001713.

Galli, P., V. Scionti, and V. Spina (2007), New paleoseismic data from the Lakes and Serre faults (Calabria, southern Italy). Seismotectonic implication, *Boll. Soc. Geol. It.*, *126*, 347–364.

Galli, P., F. Galadini, and D. Pantosti (2008), Twenty years of paleoseismology in Italy, *Earth Sci. Rev.*, *88*, 89–117.

Gerya, T. V., D. A. Yuen, and W. V. Maresch (2004), Thermomechanical modeling of slab detachment, *Earth Planet. Sci. Lett.*, *226*, 101–116.

Ghisetti, F. (1992), Fault parameters in the Messina Straits (southern Italy) and relations with the seismogenic source, *Tectonophysics*, *210*, 117–133.

Giardini, D., and M. Velonà (1991), Deep seismicity of the Tyrrhenian Sea, *Terra Nova*, *3*, 57–64.

Gignoux, M. (1913), Les formations marines pliocenes et quaternaires de l'Italie du sud et de la Sicilie, *Ann. Univ. Lyon*, *1*, 693 pp.

Giunchi, C., R. Sabadini, E. Boschi, and P. Gasperini (1996), Dynamic models of subduction: Geophysical and geological evidence in the Tyrrhenian Sea, *Geophys. J. Int.*, *126*, 555–578.

Goes, S., D. Giardini, S. Jenny, C. Hollenstein, H.G. Kahle, and A. Geiger (2004), A recent tectonic reorganization in the south-central Mediterranean, *Earth Planet. Sci. Lett.*, *226*, 335–345.

Guérémy, P. (1972), La Calabre centrale et septentrionale: Guide d'excursion gèomorphogique, *Trav. Inst. Géogr. Reims*, *10*, 1–128.

Guillaume, B., J. Martinod, L. Husson, M. Roddaz, and R. Riquelme (2009), Neogene uplift of central-eastern Patagonia: Dynamic response to active spreading-ridge subduction?, *Tectonics*, *28*, TC2009, doi:10.1029/2008TC002324.

Guillaume, B., F. Funiciello, C. Faccenna, J. Martinod, and V. Olivetti (2010), Spreading pulses of the Tyrrhenian Sea during the narrowing of the Calabrian slab, *Geology*, *38*, 819–822, doi:10.1130/G31038.1.

Gurnis, M. (1993), Phanerozoic marine inundation of continents driven by dynamic topography above subducting slabs, *Nature*, *364*, 589–593, doi:10.1038/364589a0.

Gvirtzman, Z., and A. Nur (1999), The formation of Mount Etna as the consequence of slab rollback, *Nature*, *401*, 782–785.

Gvirtzman, Z., and A. Nur (2001), Residual topography, lithospheric structure, and sunken slab in the central Mediterranean, *Earth Planet. Sci. Lett.*, *187*, 117–130.

Hager, B. H., and R. W. Clayton (1989), Constraints on the structure of mantle convection using seismic observations, flow models, and the geoid, in *Mantle Convection*, edited by W. R. Peltier, pp. 657–763, Gordon and Breach, New York.

Henderson, G. (1970), Carta geologica della Calabria, Sheet 183, Scale 1:25,000, Cassa del Mezzogiorno, Rome.

Hilde, T. W. C., and C. S. Lee (1984), Origin and evolution of the West Philippine basin: A new interpretation, *Tectonophysics*, *102*, 85–104.

Husson, L. (2006), Dynamic topography above retreating subduction zones, *Geology*, *34*, 741–744, doi:10.1130/G22436.1.

Husson, L., and Y. Ricard (2004), Stress balance above subduction zones: Application to the Andes, *Earth Planet. Sci. Lett.*, *222*, 1037–1050.

Jacques, E., C. Monaco, P. Tapponier, L. Tortorici, and T. Winter (2001), Faulting and earthquake triggering during the 1783 Calabria seismic sequence, *Geophys. J. Int.*, *147*, 499–516.

Kasten, K. A., J. Mascle, and O. L. S. Party (1988), ODP Leg 107 in the Tyrrhenian Sea: Insights into passive margin and backarc basin evolution, *Geol. Soc. Am. Bull.*, *100*, 1140–1156.

Kennett, B. L. N., E. R. Engdahl, and R. Buland (1995), Constraints on seismic velocities in the Earth from travel times, *Geophys. J. Int.*, *122*, 108–124.

Kincaid, C., and R. W. Griffiths (2003), Laboratory models of the thermal evolution of the mantle during rollback subduction, *Nature*, *425*, 58–62.

Knott, S. D., and E. Turco (1991), Late Cenozoic kinematics of the Calabrian arc, southern Italy, *Tectonics*, *10*, 1164–1172.

Lambeck, K., F. Antonioli, T. Purcell, and C. Stirling (2004), MIS 5.5 sea level in the Mediterranean and inferences on the global ice volumes during late MIS 6 and MIS 5.5, 32nd Int. Geol. Congr., Florence, Italy.

Lanzafame, G., and J. C. Bousquet (1997), The Maltese escarpment and its extension from Mt. Etna to the Aeolian Islands (Sicily): Importance and evolution of a lithosphere discontinuity, *Acta Vulcanol.*, *9*, 113–120.

Liu, L., S. Spasojević, and M. Gurnis (2008), Reconstructing Farallon plate subduction beneath North America back to the Late Cretaceous, *Science*, *322*, 934–938, doi:10.1126/science.1162921.

Lucente, F. P., L. Margheriti, C. Piromallo, and G. Barruol (2006), Seismic anisotropy reveals the long route of the slab through the western-central Mediterranean mantle, *Earth Planet. Sci. Lett.*, *241*, 517–529.

Malinverno, A., and W. Ryan (1986), Extension in the Tyrrhenian sea and shortening in the Apennines as result of arc migration driven by sinking of the lithosphere, *Tectonics*, *5*, 227–245.

Marotta, A. M., M. Fernàndez, and R. Sabadini (1998), Mantle unrooting in collisional settings, *Tectonophysics*, *296*, 31–46.

Marotta, M., R. Barzaghi, A. Borghi, and E. Spelta (2007), Gravity constraints on the dynamics of the crust-mantle system during Calabrian Subduction, *Geophys. J. Int.*, *171*, 977–985.

Mattei, M., V. Petrocelli, D. Lacava, and M. Schiattarella (2004), Geodynamic implications of Pleistocene ultrarapid vertical axis rotations in the Southern Apennines, Italy, *Geology*, *32*, 789–792, doi:10.1130/G20552.1.

Minelli, L., and C. Faccenna (2010), Evolution of the Calabrian accretionary wedge, central Mediterranean, *Tectonics*, *29*, TC4004, doi:10.1029/2009TC002562.

Mitrovica, J. X., C. Beaumont, and G. T. Jarvis (1989), Tilting of continental interiors by the dynamical effects of subduction, *Tectonics*, *8*, 1079–1094, doi:10.1029/TC008i005p01079.

Miyauchi, T., G. Dai Pra, and S. Sylos Labini (1994), Geochronology of Pleistocene marine terraces and regional tectonics in the Tyrrhenian coast of South Calabria, Italy, *Quaternario*, *7*, 17–34.

Molin, P., F. J. Pazzaglia, and F. Dramis (2004), Geomorphic expression of active tectonics in a rapidly-deforming forearc, Sila Massif, Calabria, southern Italy, *Am. J. Sci.*, *304*, 559–589.

Monaco, C., and L. Tortorici (2000), Active faulting in the Calabrian arc and eastern Sicily, *J. Geodyn.*, *29*, 407–424.

Monaco, C., P. Tapponnier, L. Tortorici, and P. Y. Gillot (1997), Late Quaternary slip rates on the Acireale-Piedimonte normal faults and tectonic origin of Mt. Etna (Sicily), *Earth Planet. Sci. Lett.*, *147*, 125–139.

Montelli, R., G. Nolet, F. A. Dahlen, G. Masters, E. R. Engdahl, and S. Hung (2004), Finite-frequency to-

mography reveals a variety of plumes in the mantle, *Science*, *303*, 338–343.

Montuori, C., G. B. Cimini, and P. Favali (2007), Teleseismic tomography of the southern Tyrrhenian subduction zone: New results from seafloor and land recordings, *J. Geophys. Res.*, *112*, B03311, doi:10.1029/2005JB004114.

Moresi, L., and V. Solomatov (1998), Mantle convection with a brittle lithosphere: thoughts on the global tectonic styles of the Earth and Venus, *Geophys. J. Int.*, *133*, 669–682.

Moretti, A. (2000), Il database delle faglie capaci della Calabria: Stato attuale delle conoscenze, in *Le Ricerche del GNDT nel Campo Della Pericolosità Sismica (1996–1999)*, edited by F. Galadini et al., pp. 219–226, Cons. Naz. Ric., Gruppo Naz. Difesa-dai Terremoti, Rome, Italy.

Neri, G., B. Orecchio, C. Totaro, G. Falcone, and D. Presti (2009), Subduction beneath southern Italy is close to ending: Results from seismic tomography, *Seismol. Res. Lett.*, *80*, 63–70.

Nicolosi, J., F. Speranza, and M. Chiappini (2006), Ultrafast oceanic spreading of the Marsili Basin, southern Tyrrhenian Sea: Evidence from magnetic anomaly analysis, *Geology*, *34*, 717–720, doi:10.1130/G22555.1.

Ogniben, L. (1973), Schema geologico della Calabria in base ai dati odierni, *Geol. Rom.*, *12*, 243–585.

Olivetti, V. (2009), Erosione e sollevamento nell'arco calabro-peloritano, Ph.D. thesis, 134 pp., Università degli Studi di Bologna, Italy.

Patacca, E., R. Sartori, and P. Scandone (1990), Tyrrhenian basin and Apenninic arcs. Kinematic relations since late Tortonian times, *Mem. Soc. Geol. It.*, *45*, 425–451.

Piana Agostinetti, N., and A. Amato (2009), Moho depth and V_p/V_s ratio in peninsular Italy from teleseismic receiver functions, *J. Geophys. Res.*, *114*, B06303, doi:10.1029/2008JB005899.

Piana Agostinetti, N., M. S. Steckler, and F. P. Lucente (2009), Imaging the subducted slab under the Calabrian Arc, Italy, from receiver function analysis, *Lithosphere*, *1*, 131–138, doi:10.1130/L49.1.

Pirazzoli, P. A., G. Mastronuzzi, J. F. Saliége, and P. Sansò (1997), Late Holocene emergence in Calabria (Italy), *Mar. Geol.*, *141*, 61–70.

Piromallo, C., and A. Morelli (2003), *P* wave tomography of the mantle under the Alpine-Mediterranean area, *J. Geophys. Res.*, *108*(B2), 2065, doi:10.1029/2002JB001757.

Piromallo, C., G. Spada, R. Sabadini, and Y. Ricard (1997), Sea level fluctuations due to subduction: The role of mantle rheology, *Geophys. Res. Lett.*, *24*, 1587–1590, doi:10.1029/97GL01561.

Piromallo, C., T. W. Becker, F. Funiciello, and C. Faccenna (2006), Three-dimensional instantaneous mantle flow induced by subduction, *Geophys. Res. Lett.*, *33*, L08304, doi:10.1029/2005GL025390.

Pysklywec, R. N., and J. X. Mitrovica (2000), Mantle flow mechanisms of epeirogeny and their possible role in the evolution of the western Canada Sedimentary Basin, *Can. J. Earth Sci.*, *37*, 1535–1548, doi:10.1139/cjes-37-11-1535.

Robustelli, G., F. Lucà, F. Corbi, T. Pelle, F. Dramis, G. Fubelli, F. Scarciglia, F. Muto, D. Cugliari (2009) Alluvial terraces on the Ionian coast of northern Calabria, southern Italy: Implications for tectonic and sea level controls, *Geomorphology*, *106*, 165–179.

Roveri, M., A. Bernasconi, M. E. Rossi, and C. Visentin (1992), Sedimentary evolution of the Luna Field Area, Calabria, Southern Italy, in *Generation, Accumulation, and Production of Europe's Hydrocarbons*, edited by A. M. Spencer, *Europ. Assoc. Petrol. Geosci. Spec. Publ.*, 2, 217–224.

Roy, M., T. H. Jordan, and J. Pederson (2009), Colorado Plateau magmatism and uplift by warming of heterogeneous lithosphere, *Nature*, *459*, 978–982, doi:10.1038/nature08052.

Royden, L. H., and L. Husson (2006) Trench motion, slab geometry, and viscous stresses in subduction systems, *Geophys. J. Int.*, *167*, 881–905.

Sartori, R., and ODP Leg Sci. Staff (1989), Drillings of ODP Leg 107 in the Tyrrhenian Sea: Tentative basin evolution compared to deformations in the surrounding chains, in *The Lithosphere in Italy: Advances in Earth Science Research*, edited by A. Boriani et al., pp. 139–156, Accad. Naz. Lincei, Rome, Italy.

Schellart, W. P. (2004), Kinematics of subduction and subduction-induced flow in the upper mantle, *J. Geophys. Res.*, *109*, B07401, doi:10.1029/2004JB002970.

Selvaggi, G., and C. Chiarabba (1995), Seismicity and *P* wave velocity image of the Southern Tyrrhenian subduction zone, *Geophys. J. Int.*, *121*, 818–826.

Seranne, M. (1999), Early Oligocene stratigraphic turnover on the west Africa continental margin: A signature of the Tertiary greenhouse-to-icehouse transition?, *Terra Nova*, *11*, 135–140.

Shackleton, N. J. (2000), The 100,000 year ice-age cycle identified and found to lag temperature, carbon dioxide, and orbital eccentricity, *Science*, *289*, 1897–1902.

Speranza, F. (1999), Paleomagnetism and the Corsica-Sardinia rotation: A short review, *Boll. Soc. Geol. It.*, *118*, 537–543.

Speranza, F., M. Mattei, L. Sagnotti, and F. Grasso (2000), Rotational differences between the northern and southern Tyrrhenian domains: Paleomagnetic constraints from the Amantea basin (Calabria, Italy), *J. Geol. Soc. London*, *157*, 327–334.

Spina, V., P. Galli, E. Tondi, S. Critelli, and G. Cello (2007), Kinematics and structural properties of an active fault zone in the Sila Massif (Northern Calabria, Italy), *Boll. Soc. Geol. It.*, *126*, 427–438.

Spina, V., E. Tondi, P. Galli, and S. Mazzoli (2009), Fault propagation in a seismic gap area (northern Calabria, Italy): Implications for seismic hazard, *Tectonophysics*, *476*, 357–369, doi:10.1016/j.tecto.2009.02.001.

Stegman, D. R., J. Freeman, W. P. Schellart, L. Moresi, and D. May (2006), Influence of trench width on subduction hinge retreat rates in 3D models of slab rollback, *Geochem. Geophys. Geosyst.*, *7*, Q03012, doi:10.1029/2005GC001056.

Stewart, I. S., A. Cundy, S. Kershaw, and C. Firth (1997), Holocene coastal uplift in the Taormina area, northeastern Sicily: Implications for the southern prolongation of the Calabrian seismogenic belt, *J. Geodyn.*, *24*, 37–50.

Stirling, C. H., T. M. Esat, M. T. McCulloch, and K. Lambeck (1995), High-precision U-series dating of corals from Western Australia and implications for the timing and duration of the last interglacial, *Earth Planet. Sci. Lett.*, *135*, 115–130.

Suhadolc, P., and G. F. Panza (1989), Physical properties of the lithosphere-asthenosphere system in Europe from geophysical data, in *The Lithosphere in Italy: Advances in Earth Science Research*, edited by A. Boriani et al., pp. 15–37, Accad. Naz. Lincei, Rome, Italy.

Tansi, C., A. Tallarico, G. Iovine, M. Folino Gallo, and G. Falcone (2005), Interpretation of radon anomalies in seismotectonic and tectonic-gravitational settings: the southeastern Crati graben (Northern Calabria, Italy), *Tectonophysics*, *396*, 181–193.

Tansi, C., F. Muto, S. Critelli, and G. Iovine (2007), Neogene-Quaternary strike-slip tectonics in the central Calabrian Arc (southern Italy), *J. Geodyn.*, *43*, 393–414.

Thomson, S. N. (1994), Fission track analysis of the crystalline basement rocks of the Oligo-Miocene late-orogenic extension and erosion, *Tectonophysics*, *238*, 331–352.

Thomson, S. N. (1998), Assessing the nature of tectonic contact using fission track thermochronology: An example from the Calabrian Arc, southern Italy, *Terra Nova*, *10*, 32–36.

Thorkelson, D. J. (1996), Subduction of diverging plates and the principles of slab window formation, *Tectonophysics*, *255*, 47–63, doi:10.1016/0040-1951(95)00106-9.

Tortorici, G., M. Bianca, G. De Guidi, C. Monaco, and L. Tortorici (2003), Fault activity and marine terracing in the Capo Vaticano area (southern Calabria) during the Middle-Late Quaternary, *Quat. Int.*, *101–102*, 269–278.

Tortorici, L. (1981), Analisi delle deformazioni fragili dei sedimenti postorogeni della Calabria settentrionale, *Boll. Soc. Geol. It.*, *100*, 291–308.

Tortorici, L., C. Monaco, C. Tansi, and O. Cocina (1995), Recent and active tectonics in the Calabrian Arc (southern Italy), *Tectonophysics*, *243*, 7–55.

Trua, T., G. Serri, and M. Marani (2003), Lateral flow of African mantle below the nearby Tyrrhenian plate: Geochemical evidence, *Terra Nova*, *15*, 433–440, doi:10.1046/j.1365 3121.2003.00509.x.

Turcotte, D. L., and G. Schubert (1982), *Geodynamics Applications of Continuum Physics to Geological Problems*, 450 pp., John Wiley, New York.

Valensise, G., and D. Pantosti (1992), A 125 Kyr long geological record of seismic source repeatibility: The Messina Straits (southern Italy) and the 1908 earthquake (MS 7 1/2), *Terra Nova*, *4*, 472–483.

Van Dijk, J. P., et al. (2000), A regional structural model for the northern sector of the Calabrian Arc (southern Italy), *Tectonophysics*, *324*, 267–320.

Wang, K., R. Wells, S. Mazzotti, R. D. Hyndman, and T. Sagiya (2003), A revised dislocation model of interseismic deformation of the Cascadia subduction zone, *J. Geophys. Res.*, *108*(B1), 2026, doi:10.1029/2001JB001227.

Wegmann, K. W., et al. (2007), Position of the Snake River watershed divide as an indicator of geodynamic processes in the greater Yellowstone region, western North America, *Geosphere*, *3*, 272–281, doi:10.1130/GES00083.1.

Westaway, R. (1993), Quaternary uplift of southern Italy, *J. Geophys. Res.*, *98*, 21,741–21,772.

Wortel, M. J. R., and W. Spakman (2000), Subduction and slab detachment in the Mediterranean-Carpathian region, *Science*, *290*, 1910–1917.

Zecchin, M., R. Nalin, and C. Rodad (2004), Raised Pleistocene marine terraces of the Crotone peninsula (Calabria, southern Italy): Facies analysis and organization of their deposits, *Sediment. Geol.*, *172*, 165–185.

Zhong, S., and M. Gurnis (1994), Controls on trench topography from dynamic models of subducted slabs, *J. Geophys. Res.*, *99*, 15,683–15,695, doi:10.1029/94JB00809.

Zhong, S., M. T. Zuber, L. N. Moresi, and M. Gurnis (2000), Role of temperature-dependent viscosity and surface plates in spherical shell models of mantle convection, *J. Geophys. Res.*, *105*, 11,063–11,082.

O. Bellier, Centre Européen de Recherche et d'Enseignement de Géosciences de l'Environnement, UMR 6635, CNRS, Université Paul Cézanne, 3 Avenue Robert-Schuman, F-13628, Aix-en-Provence, France.

A. Billi, Istituto di Geologia Ambientale e Geoingegneria, CNR, Via Salaria Km 29, 300, I-00016, Monterotondo, Rome, Italy.

C. Faccenna, F. Funiciello, P. Molin, and V. Olivetti, Dipartimento di Scienze Geologiche, Università Roma Tre, Largo San Leonardo Murialdo 1, I-00146, Rome, Italy. (faccenna@uniroma3.it)

L. Minelli, Dipartimento di Scienze della Terra, Sapienza Università di Roma, P. le A. Moro 5, I-00185, Rome, Italy.

B. Orecchio, Dipartimento di Fisica, Università della Calabria, Via Pietro Bucci, I-87036, Cosenza, Italy.

C. Piromallo, Istituto Nazionale di Geofisica e Vulcanologia, Via Nizza 128, I-00198, Rome, Italy.